UC Berkeley
UC Berkeley Previously Published Works

Title
Strangeness production as a function of charged-particle multiplicity in proton-proton collisions at s=5.02 TeV

Permalink
https://escholarship.org/uc/item/8h06p2v8

Journal
Physical Review C, 114(2)

ISSN
2469-9985

Authors
Abualrob, IJ
Acharya, S
Rinella, G Aglieri
et al.

Publication Date
2026-08-01

DOI
10.1103/xtf2-bsc9

Copyright Information
This work is made available under the terms of a Creative Commons Attribution License, available at https://creativecommons.org/licenses/by/4.0/

Peer reviewed

eScholarship.org Powered by the California Digital Library
University of California

Strangeness production as a function of charged-particle multiplicity in proton-proton collisions at $\sqrt{s} = 5.02$ TeV

I. J. Abualrob *et al.*[*]
(ALICE Collaboration)

(Received 24 November 2025; accepted 21 May 2026; published 3 August 2026)

(Multi-)strange particle production rates and transverse momentum distributions are measured at midrapidity ($|y| < 0.5$) as a function of the charged-particle multiplicity density by the ALICE experiment at the CERN Large Hadron Collider (LHC), using proton-proton collisions at a center-of-mass energy of $\sqrt{s} = 5.02$ TeV. This study extends similar studies performed at $\sqrt{s} = 7$ TeV and $\sqrt{s} = 13$ TeV to a lower-energy regime, improving the statistical precision and extending the measurement to previously unexplored low-multiplicity regions. While K^0_S, Λ, and Ξ yields can be described with a linear multiplicity dependence within uncertainties, the Ω yields follow a significantly faster than linear increasing trend. For all analyzed particles, the overall production rate is consistent with that observed at higher energy and at similar multiplicity densities. Transverse momentum distributions are observed to evolve with multiplicity. Several state-of-the-art QCD-inspired Monte Carlo models have been compared with the data, testing some recently introduced features to address the findings at higher energies. Models can qualitatively describe the transverse momentum spectra and the Λ/K^0_S spectral ratio only if collectivity is introduced in the evolution of the system.

DOI: 10.1103/xtf2-bsc9

I. INTRODUCTION

Strange hadron formation in high-energy hadronic collisions is the subject of an intense experimental study that aims at understanding the properties of quantum chromodynamics (QCD) in its nonperturbative regime. Several QCD-inspired phenomenological Monte Carlo (MC) generators can be employed to predict the relative yields of different particle species in elementary hadronic collisions, but a comprehensive quantitative phenomenological description is still missing.

In heavy-ion collisions, an enhancement in the yield of strange hadrons relative to particles containing only u and d quarks was originally proposed as a signature of quark–gluon plasma (QGP) formation [1,2]. Strangeness enhancement has been experimentally observed over the last thirty years in heavy-ion collisions, first at the CERN Super Proton Synchrotron (SPS) [3–5] and later at the BNL Relativistic Heavy Ion Collider (RHIC) [6] and at the CERN Large Hadron Collider (LHC) [7,8]. More recently, such trends have been interpreted, in the context of the Statistical Hadronization Model (SHM) description of particle production, as originating from the change in the source volume in different colliding systems [9–11]. The ALICE collaboration recently reported on the charged-particle multiplicity dependence of strange and multistrange particle production, showing a significant strangeness enhancement trend in proton-proton (pp) and proton-lead (p-Pb) collisions [12–14]. Strange particle yields are observed to be enhanced in high-multiplicity proton-proton collisions with respect to the corresponding yields measured in inclusive inelastic collisions at the same energy. In the highest-multiplicity regime, relative particle abundances were found to reach values comparable to those observed in very central heavy-ion collisions. The progression with multiplicity of particle yields was observed to be independent of the collision energy, by comparing the $\sqrt{s} = 7$ TeV and $\sqrt{s} = 13$ TeV results [14]. Moreover, transverse momentum spectra were observed to evolve toward higher average transverse momentum, $\langle p_T \rangle$, when the multiplicity density in the collision increases, a feature similar to what is observed in nucleus-nucleus interactions.

To interpret these observations, phenomenological models involving string fragmentation, typically employed in elementary leptonic and hadronic collisions [15,16], have been adapted by introducing final-state mechanisms that can enhance the number of baryons and strange particles in hadronic interactions by modifying the hadronization mechanisms in high-density environments [17–20]. At the same time, statistical models [21,22] and core-corona models [23,24] have been exploited, extending their predictions from the high-multiplicity to the low-multiplicity regime.

In this paper, we report on the study of K^0_S, Λ, $\overline{\Lambda}$, Ξ^-, $\overline{\Xi}^+$, Ω^-, and $\overline{\Omega}^+$ production, making use of the large dataset ($\mathscr{L}_{\rm int} = 2.3$ nb^{-1}) collected during the 2017 proton-proton data-taking campaign at $\sqrt{s} = 5.02$ TeV. This is the largest dataset analyzed for hadrochemistry studies in hadronic collisions, allowing for a significant improvement in the precision of the transverse momentum spectra of $\Xi^\pm$ and $\Omega^\pm$

[*]Full author list given at the end of the article.

Published by the American Physical Society under the terms of the Creative Commons Attribution 4.0 International license. Further distribution of this work must maintain attribution to the author(s) and the published article's title, journal citation, and DOI. Open access publication funded by CERN.

 ©2026 CERN, for the ALICE Collaboration

TABLE I. List of event multiplicity classes (first column), percentile intervals (second column), and corresponding charged-particle pseudorapidity densities ($|\eta| < 0.5$) for pp collisions at $\sqrt{s} = 5.02$ TeV in the INEL > 0 event class [33] for the different particles under study (K^0_S and Λ in third, Ξ in fourth and Ω in fifth column, respectively). The total systematic uncertainties are the quadratic sum of the correlated and uncorrelated systematic uncertainties.

		$\langle dN_{ch}/d\eta \rangle_{\|\eta\|<0.5}$		
Class	Multiplicity (%)	K^0_S, Λ	Ξ	Ω
I	0–0.0091	24.53 ± 0.39	22.00 ± 0.40	18.50 ± 0.17
II	0.0091–0.0915	21.71 ± 0.21		
III	0.0915–0.9152	18.11 ± 0.18	18.11 ± 0.18	
IV	0.9152–4.577	14.51 ± 0.18	14.51 ± 0.18	14.51 ± 0.18
V	4.577–9.156	11.93 ± 0.11	11.93 ± 0.11	11.24 ± 0.13
VI	9.156–13.74	9.70 ± 0.13	10.30 ± 0.13	
VII	13.74–18.32		9.12 ± 0.12	8.38 ± 0.12
VIII	18.32–27.51	7.76 ± 0.11	7.76 ± 0.11	
IX	27.51–36.76	6.34 ± 0.08	6.34 ± 0.08	5.78 ± 0.08
X	36.76–46.11	5.22 ± 0.07	5.22 ± 0.07	
XI	46.11–65.45	3.94 ± 0.06	3.94 ± 0.06	3.94 ± 0.06
XII	65.45–100	2.42 ± 0.04	2.42 ± 0.04	2.42 ± 0.04
INEL > 0	0–100		5.48 ± 0.07	

baryons. The highest possible granularity in the multiplicity slicing was favored over a larger p_T reach, allowing the measurements to be extended down to the lowest multiplicities ever probed at the LHC. In the following, particles and antiparticles are added together, as it has been demonstrated that their production yields are compatible at the LHC [12] and are hereafter referred to as Λ, Ξ, and Ω, respectively.

In Sec. II, the experimental apparatus used for the measurement is discussed, while in Secs. III and IV, the analysis technique and the evaluation of the systematic uncertainties are described, respectively. The results are presented in Sec. V, and they are compared in Sec. VI to phenomenological models. Finally, conclusions are drawn in Sec. VII.

II. EXPERIMENTAL SETUP

Details on the ALICE detectors and their performance are described in Refs. [25,26]. The detectors used for the analysis presented in this paper are the inner tracking system (ITS) [27], the time projection chamber (TPC) [28], the time-of-flight (TOF) detector [29], and the two scintillator arrays of the V0 detector [30]. The ITS, TPC, and TOF are part of the central barrel and are cylindrically arranged around the interaction point (IP), enclosed within the L3 solenoid magnet, which provides a field up to 0.5 T. Unless specified otherwise, the pseudorapidity coverage of the detectors in the central barrel is $|\eta| < 0.9$. The ITS is the detector closest to the beam pipe and the IP. It comprises six cylindrical layers of silicon micropattern detectors with a two-dimensional readout. The innermost layers, for which a higher granularity is required, are made of silicon pixel detectors (SPDs). The next two layers are covered by silicon drift detectors (SDDs), while the outer layers consist of silicon strip detectors (SSDs). The TPC is the main tracking detector in ALICE. It is a cylindrical gaseous detector with an internal volume of 88 m^3 surrounding the ITS. Its timing and spatial information provide up to 159 three-dimensional space points as well as the specific energy loss of the particles of interest. The TPC also provides particle identification through a dE/dx measurement, which covers the low-momentum region up to a few tens of GeV/c, with a resolution around 5%–7%. The outermost detector used is the TOF, positioned at a distance of 370 cm. It has full azimuthal acceptance, and an overall time resolution down to ≈60 ps, and is used to measure the time of flight. The V0 detector is made up of two scintillator hodoscopes located around the beam pipe on opposite sides of the IP at $z = +340$ cm (V0A) and $z = -90$ cm (V0C) and covers $2.8 < \eta < 5.1$ and $-3.7 < \eta < -1.7$, respectively. It provides the minimum-bias trigger and the identification and rejection of beam-gas events. Additionally, the V0A and V0C detectors (together defined as V0M) are used to determine the charged-particle multiplicity density.

III. DATA ANALYSIS

The analysis presented in this paper follows a strategy similar to the one described in previous ALICE publications [12–14,31,32]. Primary strange hadrons were measured at central rapidity ($|y| < 0.5$) in events with at least one charged particle produced in the pseudorapidity interval $|\eta| < 1$ (INEL > 0), corresponding to about 75% of the total inelastic cross section [33]. Events were required to have a reconstructed vertex within the longitudinal interval $|z| < 10$ cm from the IP, while events containing more than one distinct vertex were tagged as pileup and discarded. To study the multiplicity dependence of strange hadron production, the sample was divided into event classes based on the total charge deposited in both the V0 detectors (V0M amplitude), which is proportional to the total number of charged particles detected by the V0 scintillators. The event classes are summarized in Table I. For each class, the average primary charged-particle density $\langle dN_{ch}/d\eta \rangle_{|\eta|<0.5}$ at midrapidity was calculated, fully

TABLE II. List of selection criteria applied to particle candidates and their decay tracks for the K^0_S, Λ, Ξ, and Ω analyses.

Topological Variable	K^0_S (Λ)	Ξ (Ω)
DCA pos. (neg.) decay track to PV	>0.06 cm	>0.12 (0.13) cm
DCA V^0 decay tracks	$<1.0\,\sigma$	$<1.3\sigma$
DCA bachelor to PV		>0.04 cm
DCA V^0 to PV		>0.06 cm
DCA bachelor to V^0		<1.3 cm
DCA bachelor to baryon (only Ξ)		>0.02 cm
V^0 cosine of pointing angle	>0.97(0.995)	>0.97
cascade cosine of pointing angle		>0.97
V^0 transverse decay radius	>0.5 cm	>1.2 (1.1) cm
cascade transverse decay radius		>0.6 (0.5) cm
Candidate Selection	**K^0_S (Λ)**	**Ξ (Ω)**
rapidity interval	$\lvert y\rvert < 0.5$	$\lvert y\rvert < 0.5$
proper decay length	<20 (30) cm	<15 (7.5) cm
distance to competing cascade mass		$-$ (8 MeV/c^2)
V^0 invariant mass window		8 MeV/c^2
decay tracks with ITS refit or TOF matching	$\geqslant$1	$\geqslant$1
Track Selection	**K^0_S (Λ)**	**Ξ (Ω)**
TPC dE/dx selection	$<4\,\sigma$	$<4\,\sigma$
pseudorapidity interval	$\lvert\eta\rvert < 0.8$	$\lvert\eta\rvert < 0.8$
TPC $N_{\text{crossed}}/N_{\text{findable}}$	$\geqslant$0.8	$\geqslant$0.8
TPC $N_{\text{crossed rows}}$	$\geqslant$70	$\geqslant$70

corrected for acceptance, tracking, and vertexing efficiency as well as for contamination from secondary particles and combinatorial background. Note that the midrapidity multiplicity distribution corresponding to each V0M class has a large relative root mean square (rms), ranging from 70% to 30% for the lowest and highest multiplicity classes, respectively. More details can be found in Ref. [33].

The strange hadrons K^0_S and Λ (V^0) and Ξ and Ω (cascades) were each reconstructed via their specific weak decay topology [34]:

$$K^0_S \to \pi^+ + \pi^-, \quad \text{B.R.} = (69.20 \pm 0.05)\%,$$
$$\Lambda \to p + \pi^-(+\text{c.c.}), \quad \text{B.R.} = (63.9 \pm 0.5)\%,$$
$$\Xi^- \to \Lambda + \pi^-(+\text{c.c.}), \quad \text{B.R.} = (99.887 \pm 0.035)\%,$$
$$\Omega^- \to \Lambda + K^-(+\text{c.c.}), \quad \text{B.R.} = (67.8 \pm 0.7)\%,$$

applying a series of track, candidate, and topological selections as summarized in Table II. The selection criteria were previously discussed in detail in Ref. [14] and were optimized through specific studies performed on MC simulations.

In this analysis, ITS and TPC are the main detectors employed for reconstructing the trajectories of pions, protons, and charged kaons, which constitute the tracks generated by the weak decay of the particles under study. The reconstructed tracks, selected in the pseudorapidity region $|\eta| < 0.8$, were required to have a number of TPC crossed rows larger than 70 and a fraction of TPC crossed rows and findable clusters larger than 80%. Particle identification was performed by measuring the energy-loss per unit of track length in the TPC gas volume and requiring it to be within $\pm 4\sigma_{\mathrm{d}E/\mathrm{d}x}$ from the expected calculated average using the Bethe–Bloch parametrization, where $\sigma_{\mathrm{d}E/\mathrm{d}x}$ is the $\mathrm{d}E/\mathrm{d}x$ resolution.

Topological selections were applied to the reconstructed weak decay candidates to reduce the combinatorial background. The distance of closest approach (DCA) between the V^0 decay tracks was required to be smaller than 1 (1.3) standard deviation in the V^0 (cascades) analyses. The DCA between each V^0 decay track and the primary collision vertex (PV) was required to be larger than 0.06 (0.12 or 0.13) cm for the V^0 (Ξ or Ω) analyses. For the cascades, the DCA between the bachelor track (charged track from the first weak decay) and the primary vertex was required to be larger than 0.04 cm, the DCA between the V^0 and the primary vertex was larger than 0.06 cm, while the DCA between the bachelor track and V^0 was smaller than 1.3 cm. In the Ξ analysis, an additional cut on the minimum DCA between the bachelor track and the baryon V^0 decay track was applied (0.02 cm) to avoid the inclusion of candidates for which a decay product from the V^0 meson was incorrectly assigned as the bachelor track. The cosine of the angle between the candidate momentum and the vector connecting the primary and secondary vertices (pointing angle) was required to be larger than 0.97 for each case except for the Λ, for which a stricter cut of 0.995 was applied. The radial distance between the PV and the V^0 vertex was set to be larger than 0.5 (1.2 or 1.1) cm for the V^0 (Ξ or Ω) analyses, while in the cascade analysis, an additional requirement on the minimum transverse decay radius for the secondary vertex was defined at 0.6 (0.5) for Ξ (Ω). Reconstructed candidates were retained if the proper decay length was measured to be smaller than 20, 30, 15, and 7.5 cm for the K^0_S, Λ, Ξ, and Ω analyses, respectively. The V^0 candidates from cascade decays were required to match an invariant-mass window of ± 8 MeV/c^2 with respect to the nominal Λ mass. In the Ω analysis, an additional selection on the invariant mass starting from the alternative cascade hypothesis was implemented, requiring it to be separated by more than 8 MeV/c^2 from the nominal Ξ mass. To reduce effects due to out-of-bunch pileup on the measured yields, it was required that at least one of the decay tracks either had a measured signal in the TOF detector or was reconstructed in both the ITS and TPC detectors.

Signal extraction from the invariant-mass distribution of each candidate in p_{T} and multiplicity intervals was performed as previously detailed in Refs. [12–14]. A preliminary fit of the invariant-mass distribution was performed using a Gaussian for the signal peak plus a second-order polynomial function to describe the background. This allowed for extracting the mean (μ) and width (σ) of the peak and modeling the background. The signal was then extracted with a bin counting procedure in a mass range within $\pm 5\sigma$ with respect to μ, subtracting the integral of the background fit function in the same mass window.

Λ yields are affected by significant contamination from secondary particles, coming from the decay of charged and neutral Ξ. To estimate this contribution, the charged Ξ spectra (twice the particle or antiparticle spectrum to account for the neutral Ξ decay, assuming $\Xi^{-(+)}/\Xi^0 = 1$) were folded with an MC-based p_{T}-binned two-dimensional (2D) matrix describing the decay kinematics and incorporating secondary Λ reconstruction efficiencies. Further details on MC simulations can be found below. The fraction of secondary Λ particles in the measured spectrum varied between 10% and 20%, depending on p_{T} and multiplicity.

Raw p_{T} distributions were corrected for detector acceptance and efficiency, estimated using MC simulated events featuring the PYTHIA 8 generator [15] and GEANT 3 [35] transport code for the propagation through the detector material. Use of GEANT 4 [36] was also tested, showing no significant difference compared with the default code. The acceptance-times-efficiency was found to change with p_{T}, reaching values of about 40%, 30%, 30%, and 20% at intermediate p_{T} for $\mathrm{K}^0_{\mathrm{S}}$, Λ, Ξ, and Ω, respectively. These values include the branching-ratio factors. They are observed to be independent of the multiplicity class to within 2%, a value limited by the available MC simulated data. The dependence of the efficiency on the generated p_{T} distributions was checked for all particle species. This effect, only relevant when large p_{T} intervals are considered (Ξ and Ω analyses), was removed by reweighting the MC p_{T} distribution in order to adapt it to the measured one using a rapidly converging iterative procedure. The normalization factor for the INEL > 0 event class was corrected to account for events lost due to trigger inefficiency [33]. Untriggered events may also contain signal candidates, so that a p_{T}-dependent correction was estimated by exploiting the same MC simulations used for the evaluation of acceptance and efficiency.

To compute average p_{T} ($\langle p_{\mathrm{T}} \rangle$) and the p_{T}-integrated production yields, the spectra were fitted with a Lévy-Tsallis [37,38] function to extrapolate the unmeasured p_{T} region down to $p_{\mathrm{T}} = 0$. To avoid potential bias coming from the fit of large p_{T} bins in the cascades analysis, and at high p_{T}, the integral of the function was fitted to the bin contents. The systematic uncertainties for this extrapolation procedure were evaluated using other fit functions, as discussed in the next section.

IV. SYSTEMATIC UNCERTAINTIES

Several sources of systematic uncertainties were considered, following the strategy previously reported in Ref. [14]. To avoid being limited by the MC sample size in the systematic uncertainty determination and since systematics were shown to be independent of multiplicity, the INEL > 0 class was used, and the same relative systematic uncertainty was assigned to all multiplicity classes. The stability of the signal extraction method was tested by varying the width used to define the "signal" region, expressed in terms of the number of σ (see Sec. III), varying it from the default $\pm 5\sigma$ to $\pm 4\sigma$ and $\pm 6\sigma$. This uncertainty, moderately p_{T} dependent, was below 1% for $\mathrm{K}^0_{\mathrm{S}}$ and below 2% for all other particles. Acceptance and efficiency corrections can introduce a systematic bias if the track, candidate, and topological selections differ in MC from real data. This uncertainty was estimated by varying all the selection criteria within ranges, leading to a maximum variation of $\pm 10\%$ in the raw signal yield. The results were compared with those obtained with the default selection criteria, considering a significant variation which is incompatible with statistical fluctuations following the prescription in Ref. [39] with a 1σ threshold. Significant variations, induced by each selection separately, were added in quadrature to evaluate the systematic uncertainty. The resulting uncertainty from topological, candidate, and track selections depends on p_{T} and amounts at most (at low p_{T}) to 1.5%, 5%, 6%, and 4.5% for $\mathrm{K}^0_{\mathrm{S}}$, Λ, Ξ, and Ω, respectively. Furthermore, a 2% uncertainty was added in quadrature to account for possible variations of the efficiency with multiplicity. The uncertainty due to the approximate knowledge and description of the detector material was estimated with an MC simulation, where the material budget was varied within its uncertainty of $\pm 4.5\%$ [14]. The assigned systematic uncertainty ranges from 8% to 1% at low and high p_{T} for cascades, while it stays below 4% for $\mathrm{K}^0_{\mathrm{S}}$ and Λ.

While in-bunch pileup rejection turns out to have a negligible effect for the data-taking period under study (the probability of having more than one pp interaction in a bunch crossing is $\approx 10^{-3}$), out-of-bunch pileup rejection was necessary and implemented by requiring ITS or TOF matching (see Sec. III). The systematic uncertainty for this rejection procedure was evaluated by requiring both (or at least two for cascades) daughter tracks to be reconstructed in the ITS or TOF. The difference from the default case was taken as the systematic uncertainty, which is found to increase with p_{T} and saturate at high p_{T}, reaching a maximum value of 3%.

In the Λ analysis, the feed-down correction method is a source of systematic uncertainty, due to the uncertainties of the measured Ξ spectrum and the assumption that the Λ originates in equal amounts from neutral and charged Ξ. The measured cascade spectra were moved upward and downward by 1σ in the systematic uncertainty, followed by a reevaluation of the feed-down. Moreover, the assumption of $\Xi^{\pm}/\Xi^0 = 1$ was replaced by the ratio extracted from the same MC simulation used to evaluate the acceptance and efficiency correction. The total difference with respect to the standard approach ranges from 2% to 5%, depending on p_{T} and multiplicity. Systematics related to the normalization of the corrected spectra were evaluated using the EPOS-LHC MC instead of the default PYTHIA 8 simulations. The systematic errors obtained do not exceed 4% at low multiplicity for all particles, and they rapidly become negligible as the multiplicity increases.

The $\langle p_{\mathrm{T}} \rangle$ and integrated yields for all particles except for the $\mathrm{K}^0_{\mathrm{S}}$ were obtained from the extrapolation to the unmeasured region. This procedure leads to an additional systematic uncertainty due to the unknown functional form used to reproduce the extended p_{T} spectrum. As illustrated in Sec. III, a default extrapolation was performed using the Lévy-Tsallis formula, which describes the p_{T} spectra for all the examined strange hadrons over the full measured p_{T} range. The uncertainty for the extrapolated fraction was estimated by fitting the spectra with four alternative functions

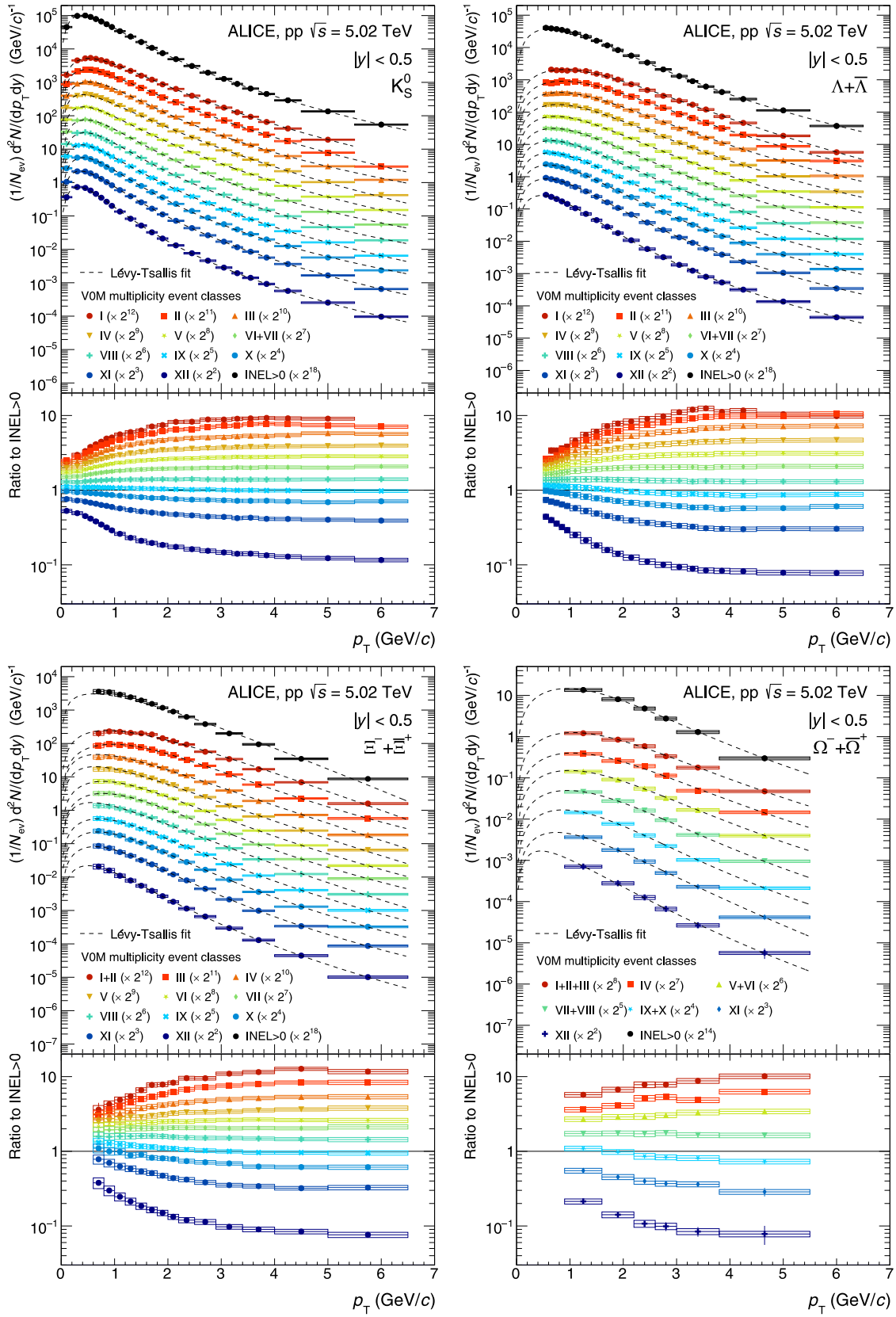


FIG. 1. p_T distributions at midrapidity for K^0_S, Λ, Ξ, and Ω for multiplicity classes and INEL > 0, as indicated. Statistical uncertainties are shown as error bars, the systematic ones as boxes. The bottom panels present the ratio of all spectra to the INEL > 0 one. The dashed curves show the Lévy-Tsallis [37] fit to the p_T distributions.

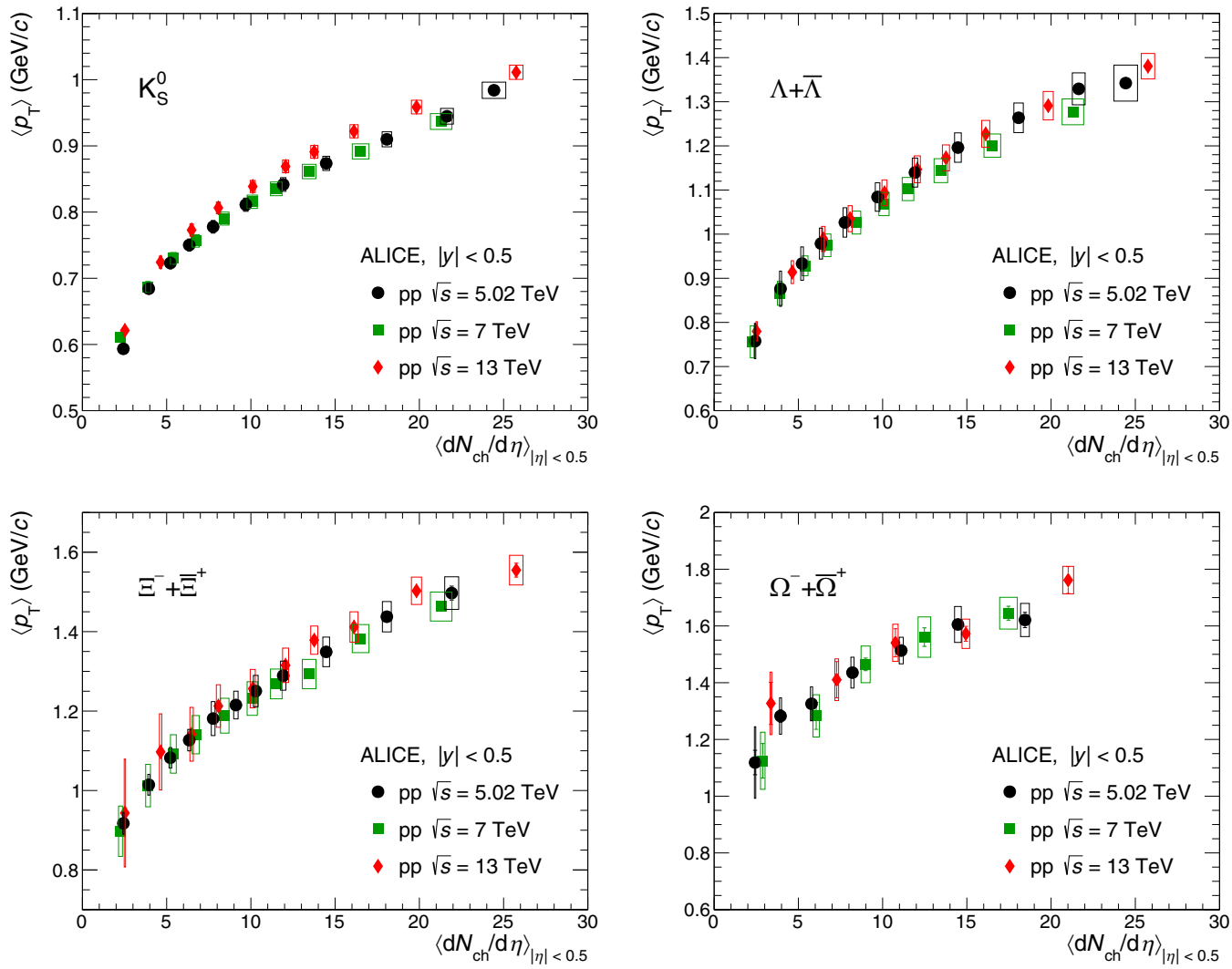


FIG. 2. $\langle p_T \rangle$ in pp collisions at different center-of-mass energies and midrapidity as a function of the event multiplicity for K^0_S and Λ (top panels), Ξ and Ω (bottom panels). $\sqrt{s} = 5.02$ TeV results are shown as black dots, $\sqrt{s} = 7$ TeV results [13] as green squares, and $\sqrt{s} = 13$ TeV results [14] as red diamonds. Statistical uncertainties are reported as error bars, systematic uncertainties as boxes whose width represents the systematic error on the multiplicity determination.

(Blast-Wave, Boltzmann, m_T-exponential, Fermi-Dirac). The resulting uncertainty for the integrated yields largely depends on multiplicity, ranging from 7% at low multiplicity to 2.5% at high multiplicity for Λ, from 13% to 1% for Ξ and from 17% to 3% for Ω. The extrapolation uncertainty for $\langle p_T \rangle$ is generally smaller, approximately half of that for the yields.

V. RESULTS

The p_T distributions of K^0_S, Λ, Ξ, and Ω for each multiplicity class and the multiplicity-integrated case are shown in Fig. 1 together with the fit performed with a Lévy-Tsallis distribution. The p_T spectra feature a maximum which moves toward larger values as the multiplicity increases, a feature previously observed in large colliding systems and interpreted as the result of a collective boost in the radial direction. This feature is highlighted in the lower panels of Fig. 1, where the ratio of the multiplicity-differential spectrum to the INEL > 0 is reported for all particles under study. These ratios evolve significantly at low p_T, approaching a plateau at around 4 GeV/c, where they saturate for K^0_S and Λ. For the first time in pp collisions, the precision achieved with the present measurement allows such a saturation region to be approached for multistrange hadrons as well, although measurements at even higher p_T would be necessary to strengthen the observation.

To quantify the evolution of the low-p_T region of the spectra with multiplicity, the $\langle p_T \rangle$ is presented in Fig. 2. These values are compared with those obtained at higher energies in pp collisions by the ALICE Collaboration [12,14]. The increasing trend of $\langle p_T \rangle$ is consistent for all center-of-mass energies, except for a 1σ difference for the K^0_S, for which results at the highest energy tend to be higher over the full multiplicity range.

Another interesting observable that quantifies the multiplicity evolution of the p_T distributions is the ratio of the

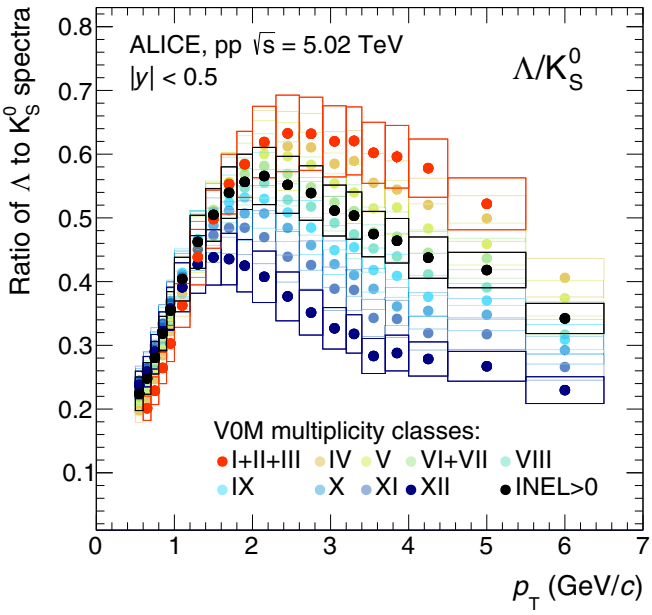


FIG. 3. p_T distribution of Λ/K^0_S ratio in pp collisions at $\sqrt{s} =$ 5.02 TeV and midrapidity for different multiplicity classes are shown with different colors. The lowest, highest, and the INEL > 0 classes are highlighted.

Λ and K^0_S spectra for each multiplicity class. This ratio is expected to evolve with multiplicity as the radial push experienced by baryons should be larger than that experienced by mesons if a collective medium is formed. Figure 3 shows the p_T evolution of the Λ/K^0_S ratio for different multiplicity classes. Highlighted are the lowest, highest, and INEL > 0 multiplicity classes. The ratio increases at low p_T, reaches a maximum between 1.5 and 3 GeV/c and then descends toward higher p_T. The position of the maximum evolves with multiplicity, being highest for the collisions with the highest multiplicity. The INEL > 0 ratio follows the lowest multiplicity trend at very low p_T and then reaches higher values toward the highest multiplicity classes. This reflects the basic fact that the INEL > 0 spectra are dominated by low-multiplicity events at low p_T (where the spectra are softer) and by higher-multiplicity events at higher p_T (where the spectra are harder).

Integrated yields are presented in Fig. 4. The multiplicity progression is also compared with results at higher pp energies, showing an excellent agreement of all three pp energies. This demonstrates that the collision center-of-mass energy at the LHC does not affect strange particle production yields when similar multiplicities are at play. It was proposed [40] that the overall multiplicity evolution of the strange-particle over pion ratio may be fully determined by the minimum multiplicity necessary to produce one strange meson or baryon (pedestal effect). This interpretation starts from the observation that the dN/dy dependence on multiplicity is approximately linear, which can now be tested with higher precision based on the present results. In Fig. 4, the dashed lines show the result of a linear combined fit to the experimental results at all center-of-mass energies, considering a quadratic sum of statistical and total systematic uncertainties. Systematic uncertainties are treated as uncorrelated across multiplicity, as a comprehensive assessment of their correlation with multiplicity is currently unavailable. A combined test of χ^2 and Wald-Wolfowitz runs [41] shows that the trend is linear for K^0_S, Λ, and Ξ (p-value > 0.3 in all cases). For the Ω baryon, instead of a linear fit (p-value $\approx 8 \times 10^{-5}$), a quadratic trend describes the data better (dotted line, p-value $= 0.6$). Note that, despite its better reproduction of the pp multiplicity ranges, the quadratic trend does not hold at multiplicities typical of p-Pb and Pb-Pb interactions, as the trend of the ratio to pions would not saturate at the highest multiplicity, as was previously observed by ALICE [8]. The intercept of the linear fit with the x axis (event multiplicity), the so-called "pedestal" (P) [40], was estimated for the different strange hadrons to be $P_{K^0_S} = 0.09 \pm 0.02$ (stat.) ± 0.40 (syst.), $P_\Lambda = 0.30 \pm 0.03$ (stat.) ± 0.72 (syst.), $P_\Xi = 1.79 \pm 0.09$ (stat.) ± 0.56 (syst.), $P_\Omega = 3.80 \pm 0.14$ (stat.) ± 0.58 (syst.).

VI. COMPARISON TO PHENOMENOLOGICAL MODELS

The reported results can be compared with state-of-the-art general-purpose Monte Carlo generators, such as PYTHIA, EPOS 4, and DCCI.

PYTHIA [15] is a phenomenological model incorporating pQCD processes and hadronization through color string fragmentation [42]. The "PYTHIA 8 Monash 2013" tune, widely used in high-energy physics, implements multiple-parton interactions (MPI) and a basic version of the Color Reconnection (CR) mechanism [43], which are both essential to reproduce the large variety of charged-particle multiplicity densities and p_T spectral shapes of unidentified hadrons measured in high-energy hadronic collisions. LHC results of identified particle production as a function of the multiplicity density necessitated the inclusion of more sophisticated CR mechanisms, implementing QCD-allowed three-leg junctions [17], and a modified string tension model in dense QCD environments, the so-called "ropes" mechanism [19]. This more recent version of the PYTHIA model will hereafter be called "PYTHIA 8 QCD-CR+Ropes."

EPOS 4 [44–46] is the newest version of the widely used EPOS model, based on the Gribov-Regge theory at parton level [47]. Collective effects and modified hadronization in high-multiplicity environments are obtained by means of the "core-corona" mechanism [23], which includes two different hadronization regimes: a high-density one (core), implementing statistical hadronization and hydrodynamic expansion, and an in-vacuum one (corona), which features string fragmentation. In the newest version of the model, some important phenomenological issues like energy conservation, factorization, and saturation are implemented in a consistent way.

The dynamical core-corona initialization model (DCCI) [48] is a state-of-the-art implementation of the core-corona approach [24]. In this case, the evolution of the system in its core and corona regions is dynamic, driven by the collisions that each parton experiences throughout the time evolution. Finally, hadronization can occur in vacuum (using PYTHIA) or using the Cooper-Frye formula from core droplets.

In the models, multiplicity classes are defined as percentiles of the multiplicity distribution in the V0M geometrical acceptance region, adapting the class boundaries to match

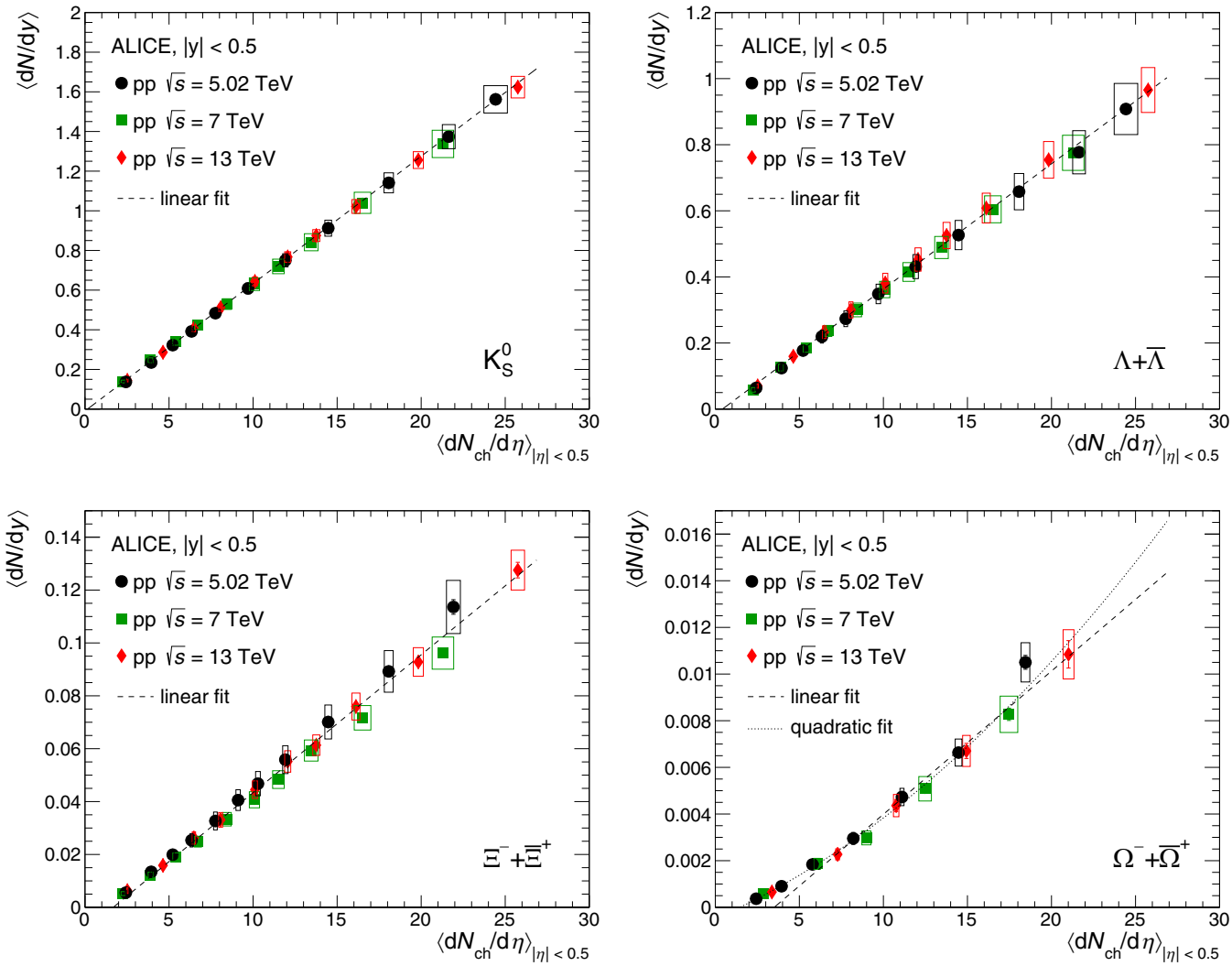


FIG. 4. p_{T}-integrated yields in pp collisions at different center-of-mass energies and midrapidity as a function of the event multiplicity for $\mathrm{K}^0_{\mathrm{S}}$ and Λ (top panels), Ξ and Ω (bottom panels). $\sqrt{s} = 5.02$ TeV results are shown as black dots, $\sqrt{s} = 7$ TeV results [13] as green squares and $\sqrt{s} = 13$ TeV results [14] as red diamonds. Statistical uncertainties are represented as error bars and systematic uncertainties as boxes whose width represents the systematic error on the multiplicity determination. Linear combined fits are shown as dashed lines, while the quadratic fit to the Ω progression is shown as a dotted line.

the corresponding $\langle \mathrm{d}N_{\mathrm{ch}}/\mathrm{d}\eta \rangle_{|\eta|<0.5}$ values measured from the data. No extrapolation is necessary to extract yields and $\langle p_{\mathrm{T}} \rangle$ for the models, as their transverse momentum spectra extend to zero p_{T}.

Figure 5 reports the comparison of particle yields and $\langle p_{\mathrm{T}} \rangle$ to the aforementioned MC generators. The improvement in the prediction of particle yields, when introducing QCD-inspired CR and the Ropes mechanism in PYTHIA, is noticeable for baryons, while the effect on mesons is negligible. The improvement, on the other hand, is absent with regards to the $\langle p_{\mathrm{T}} \rangle$, where the increasing trend with multiplicity is better reproduced by the QCD-CR+Ropes tuning, but the spectra are overall softer in the model by about 20%. EPOS 4 provides a rather good description of the yields (slightly overshooting the $\mathrm{K}^0_{\mathrm{S}}$ and Ω trends) and a satisfactory description of $\langle p_{\mathrm{T}} \rangle$ for baryons (with some tension for Ω at high multiplicity), while for $\mathrm{K}^0_{\mathrm{S}}$ the EPOS 4 spectra are softer compared with the data across all multiplicities. The DCCI model underpredicts the trend of the baryon yields with multiplicity, while slightly overshooting the one of $\mathrm{K}^0_{\mathrm{S}}$. On the other hand, it describes the $\langle p_{\mathrm{T}} \rangle$ rather well for all particles, except for $\mathrm{K}^0_{\mathrm{S}}$ at very high multiplicity. In general, although none of these models quantitatively describes both observables simultaneously for all strange hadrons, EPOS 4 provides the most accurate description for baryons. Note that the compatibility of the multiplicity trend of yields extracted at different $\sqrt{s}$ implies that the success of statistical model fits at higher energies [22] would reflect in a very good comparison in the left column of Fig. 5

The $\Lambda/\mathrm{K}^0_{\mathrm{S}}$ ratio is compared with the aforementioned MC generators in Fig. 6 for the lowest- and highest-multiplicity classes (left and right panels) and for the INEL > 0 class (central panel). Considering the PYTHIA 8 generator, the improvement introduced by the advanced CR model is again

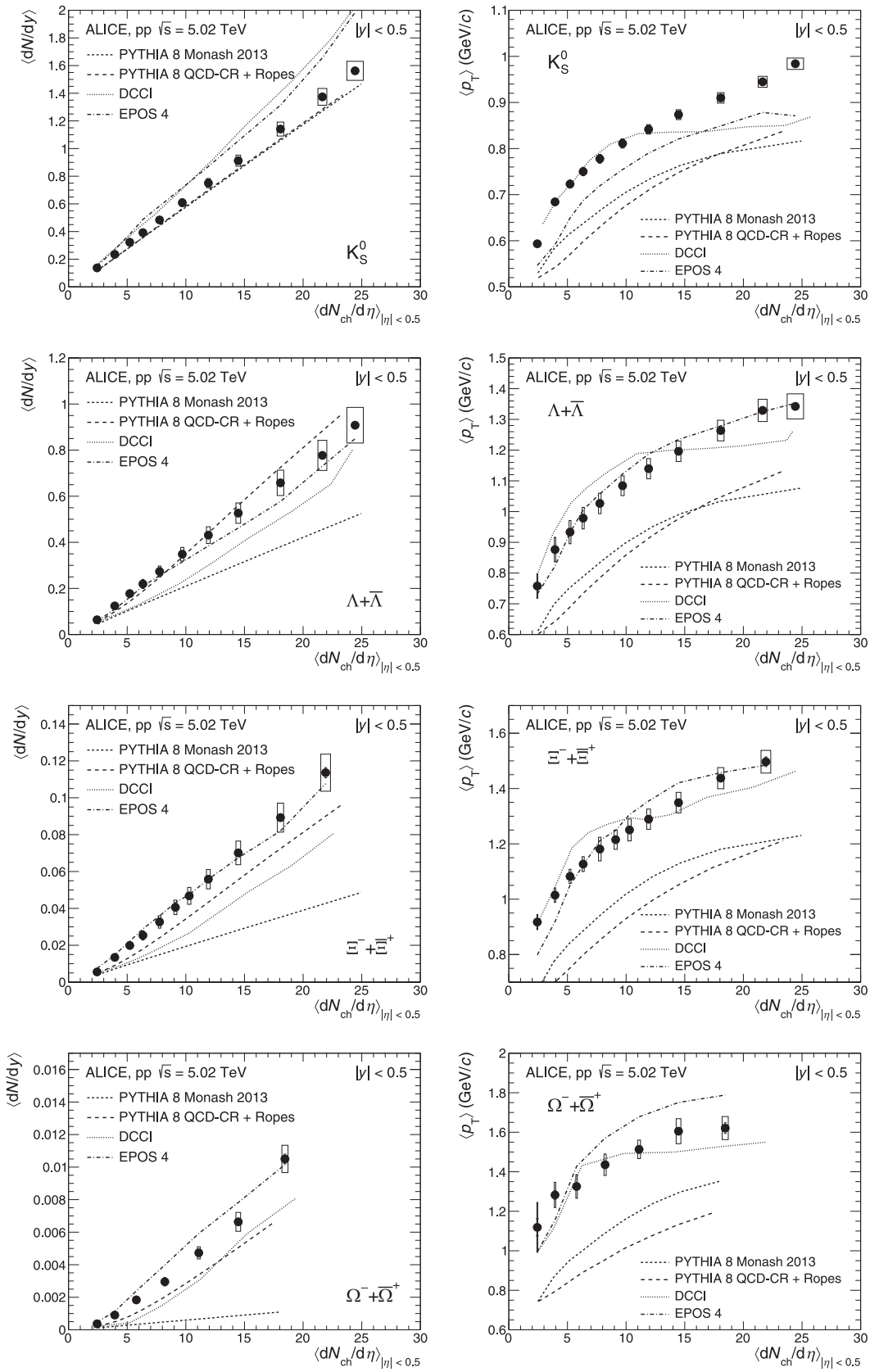


FIG. 5. p_{T}-integrated yields (left column) and $\langle p_{\mathrm{T}} \rangle$ (right column) at $\sqrt{s} = 5.02$ TeV for $\mathrm{K}^0_{\mathrm{S}}$, Λ, Ξ, and Ω compared with MC generators PYTHIA 8 Monash 2013 (Ref. [43], dashed line), PYTHIA 8 QCD-CR+Ropes (Ref. [19], long-dashed line), DCCI (Ref. [24], dotted line) and EPOS 4 (Ref. [46], dash-dotted line).

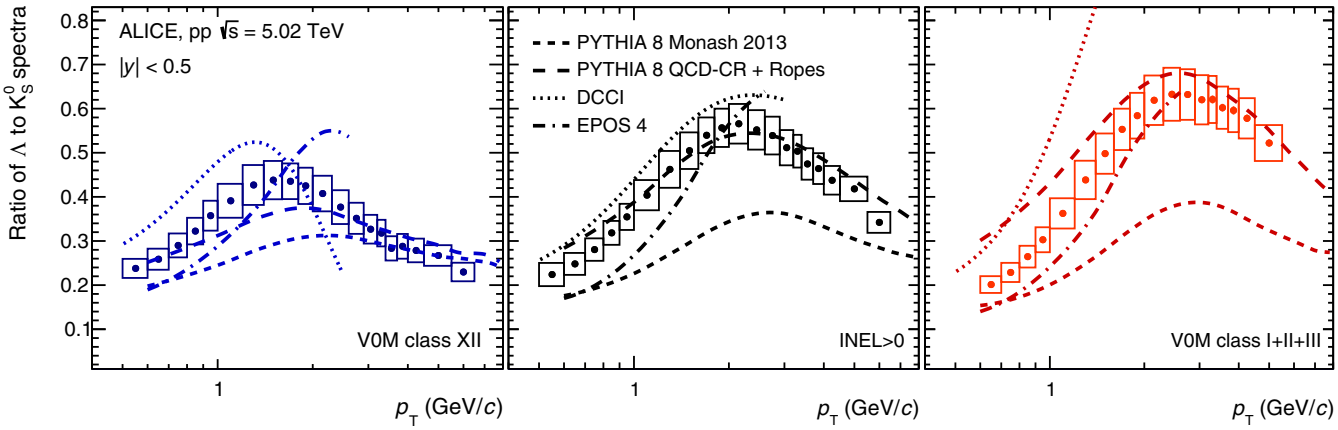


FIG. 6. p_{T} distribution of $\Lambda/\mathrm{K}^0_{\mathrm{S}}$ ratio in the INEL > 0 event class (center) and low and high-multiplicity classes (left and right panels, respectively) from pp collisions at $\sqrt{s} = 5.02$ TeV. Data are compared with PYTHIA 8 Monash 2013 (dashed lines), PYTHIA 8 QCD-QR+Ropes (long-dashed lines), DCCI (dotted lines), and EPOS 4 (dash-dotted lines) MC generators.

evident in predicting the maximum observed in the data at intermediate p_{T}. The Monash 2013 tune underpredicts all ratios and does not describe the shift of the peak with multiplicity. By contrast, the QCD-CR+Ropes tune improves the agreement with the data substantially, limiting the discrepancy to the very-low-p_{T} region, where the model underpredicts (overpredicts) at low (high) multiplicity, while the agreement in the INEL > 0 case is satisfactory. EPOS 4 has a reasonable agreement with the observed trend for INEL > 0 and at high multiplicity, but deviates at low multiplicity, where the model shows significant tensions both in the magnitude of the effect and in the position of the peak. The DCCI model fails to predict the evolution of ratios with multiplicity: although the description of the INEL > 0 ratio is satisfactory, the low and high multiplicities show large incompatibilities. Both the EPOS 4 and DCCI model curves terminate at 2.5 GeV/c to avoid large fluctuations due to limited statistics.

In general, all comparisons show that the data can be qualitatively described only if certain aspects of parton collectivity and modified hadronization in high-multiplicity collisions are considered and introduced in the models. Whether collectivity should be considered as parton flow (as in the two-component models EPOS 4 and DCCI) or Color Reconnection (as in PYTHIA) remains an open issue. Similarly, hadron yields can only be described if modified hadronization in a parton-dense environment is introduced: thermal hadronization is implemented in the case of EPOS 4 and DCCI, while color reconnection and ropes account for the description of the observed yields in a model like PYTHIA.

VII. CONCLUSIONS

The production of strange ($\mathrm{K}^0_{\mathrm{S}}$ and Λ) and multistrange (Ξ and Ω) hadrons was studied as a function of multiplicity in pp collisions at $\sqrt{s} = 5.02$ TeV, exploiting a large data sample collected by the ALICE experiment during LHC Run 2.

Transverse momentum spectra, measured with unprecedented precision, show a distinctive hardening moving toward high multiplicity. The evolution stops at around 4 GeV/c, after which the ratio of the multiplicity selected to the INEL > 0 spectra approaches a saturation region. The evolution of the spectra was quantitatively studied by extracting the $\langle p_{\mathrm{T}} \rangle$ and the $\Lambda/\mathrm{K}^0_{\mathrm{S}}$ ratio. The $\langle p_{\mathrm{T}} \rangle$ increases with multiplicity, a feature that can be reproduced by phenomenological models only if certain aspects of collectivity at the partonic level are introduced. The $\Lambda/\mathrm{K}^0_{\mathrm{S}}$ ratio features a structure with an intermediate-p_{T} maximum, which is reminiscent of the more prominent one observed in larger collision systems. Also in this case, models can qualitatively describe this ratio only if collectivity is introduced in the evolution of the system.

Particle yields were also studied and presented, extending previous works to lower energy (hence at slightly lower multiplicity) as well as improving the precision and granularity in the multiplicity selection, especially for multistrange baryons. Yields are observed to increase with multiplicity, in excellent agreement with what is observed at higher energies, demonstrating and confirming that the collision energy does not affect the average production probability of strange particles, whenever similar multiplicities are considered. The increase with multiplicity is consistent with a linear trend for $\mathrm{K}^0_{\mathrm{S}}$, Λ, and Ξ, while a quadratic dependence better accommodates the Ω results. Such an increase is, however, not suited to describe the Ω yields at higher multiplicities, which are accessed in p-Pb and Pb-Pb collisions. Models incorporating modified hadronization in high-density pp collisions qualitatively describe the data, whereas pure in-vacuum hadronization does not provide a good agreement.

ACKNOWLEDGMENTS

The ALICE Collaboration would like to thank all its engineers and technicians for their invaluable contributions to the construction of the experiment and the CERN accelerator teams for the outstanding performance of the LHC complex. The ALICE Collaboration gratefully acknowledges the resources and support provided by all Grid centres and the Worldwide LHC Computing Grid (WLCG) collaboration. The ALICE Collaboration acknowledges the following funding agencies for their support in building and running the ALICE detector: A. I. Alikhanyan National Science

Laboratory (Yerevan Physics Institute) Foundation (ANSL), State Committee of Science and World Federation of Scientists (WFS), Armenia; Austrian Academy of Sciences, Austrian Science Fund (FWF): [M 2467-N36] and Nationalstiftung für Forschung, Technologie und Entwicklung, Austria; Ministry of Communications and High Technologies, National Nuclear Research Center, Azerbaijan; Rede Nacional de Física de Altas Energias (Renafae), Financiadora de Estudos e Projetos (Finep), Fundação de Amparo à Pesquisa do Estado de São Paulo (FAPESP) and The São Paulo Research Foundation (FAPESP), Brazil; Bulgarian Ministry of Education and Science, within the National Roadmap for Research Infrastructures 2020–2027 (object CERN), Bulgaria; Ministry of Education of China (MOEC), Ministry of Science & Technology of China (MSTC) and National Natural Science Foundation of China (NSFC), China; Ministry of Science and Education and Croatian Science Foundation, Croatia; Centro de Aplicaciones Tecnológicas y Desarrollo Nuclear (CEADEN), Cubaenergía, Cuba; Ministry of Education, Youth and Sports of the Czech Republic, Czech Republic; The Danish Council for Independent Research | Natural Sciences, the VILLUM FONDEN and Danish National Research Foundation (DNRF), Denmark; Helsinki Institute of Physics (HIP), Finland; Commissariat à l'Energie Atomique (CEA) and Institut National de Physique Nucléaire et de Physique des Particules (IN2P3) and Centre National de la Recherche Scientifique (CNRS), France; Bundesministerium für Forschung, Technologie und Raumfahrt (BMFTR) and GSI Helmholtzzentrum für Schwerionenforschung GmbH, Germany; General Secretariat for Research and Technology, Ministry of Education, Research and Religions, Greece; National Research, Development and Innovation Office, Hungary; Department of Atomic Energy Government of India (DAE), Department of Science and Technology, Government of India (DST), University Grants Commission, Government of India (UGC) and Council of Scientific and Industrial Research (CSIR), India; National Research and Innovation Agency - BRIN, Indonesia; Istituto Nazionale di Fisica Nucleare (INFN), Italy; Japanese Ministry of Education, Culture, Sports, Science and Technology (MEXT) and Japan Society for the Promotion of Science (JSPS) KAKENHI, Japan; Consejo Nacional de Ciencia (CONACYT) y Tecnología, through Fondo de Cooperación Internacional en Ciencia y Tecnología (FONCICYT) and Dirección General de Asuntos del Personal Academico (DGAPA), Mexico; Nederlandse Organizatie voor Wetenschappelijk Onderzoek (NWO), Netherlands; The Research Council of Norway, Norway; Pontificia Universidad Católica del Perú, Peru; Ministry of Science and Higher Education, National Science Center and WUT ID-UB, Poland; Korea Institute of Science and Technology Information and National Research Foundation of Korea (NRF), Republic of Korea; Ministry of Education and Scientific Research, Institute of Atomic Physics, Ministry of Research and Innovation and Institute of Atomic Physics and Universitatea Nationala de Stiinta si Tehnologie Politehnica Bucuresti, Romania; Ministerstvo skolstva, vyskumu, vyvoja a mladeze SR, Slovakia; National Research Foundation of South Africa, South Africa; Swedish Research Council (VR) and Knut & Alice Wallenberg Foundation (KAW), Sweden; European Organization for Nuclear Research, Switzerland; Suranaree University of Technology (SUT), National Science and Technology Development Agency (NSTDA) and National Science, Research and Innovation Fund (NSRF via PMU-B B05F650021), Thailand; Turkish Energy, Nuclear and Mineral Research Agency (TENMAK), Turkey; National Academy of Sciences of Ukraine, Ukraine; Science and Technology Facilities Council (STFC), United Kingdom; National Science Foundation of the USA of America (NSF) and US Department of Energy, Office of Nuclear Physics (DOE NP), United States of America. In addition, individual groups or members have received support from: Czech Science Foundation (Grant No. 23-07499S), Czech Republic; FORTE project, reg. no. CZ.02.01.01/00/22_008/0004632, Czech Republic, co-funded by the European Union, Czech Republic; European Research Council (Grant No. 950692), European Union; Deutsche Forschungs Gemeinschaft (DFG, German Research Foundation) "Neutrinos and Dark Matter in Astro- and Particle Physics" (Grant No. SFB 1258), Germany; CONVECS project, CUP C97H23001700002 FESR 2021–2027 program, Italy; FAIR - Future Artificial Intelligence Research, funded by the NextGenerationEU program (Italy).

DATA AVAILABILITY

The data that support the findings of this article are openly available [49].

[1] J. Rafelski and B. Muller, Strangeness production in the quark - gluon plasma, Phys. Rev. Lett. **48**, 1066 (1982); **56**, 2334(E) (1986).

[2] J. Rafelski and R. Hagedorn, From hadron gas to quark matter, 2, in *International Symposium on Statistical Mechanics of Quarks and Hadrons, Bielefeld, Germany*, CERN-TH-2969 (1981), pp. 253–272.

[3] E. Andersen *et al.* (WA97 Collaboration), Strangeness enhancement at mid-rapidity in Pb Pb collisions at 158 *A* GeV/*c*, Phys. Lett. B **449**, 401 (1999).

[4] S. V. Afanasiev *et al.* (NA49 Collaboration), Cascade and anti-cascade+ production in central Pb + Pb collisions at 158GeV/c per nucleon, Phys. Lett. B **538**, 275 (2002).

[5] F. Antinori *et al.* (NA57 Collaboration), Strangeness enhancements at central rapidity in 40 *A* GeV/*c* Pb-Pb collisions, J. Phys. G **37**, 045105 (2010).

[6] B. I. Abelev *et al.* (STAR Collaboration), Enhanced strange baryon production in Au + Au collisions compared to $p+p$ at $\sqrt{s_{NN}} = 200$ GeV, Phys. Rev. C **77**, 044908 (2008).

[7] S. Acharya *et al.* (ALICE Collaboration), The ALICE experiment: A journey through QCD, Eur. Phys. J. C **84**, 813 (2024).

[8] B. B. Abelev *et al.* (ALICE Collaboration), Multi-strange baryon production at mid-rapidity in Pb-Pb collisions at $\sqrt{s_{NN}} = 2.76$ TeV, Phys. Lett. B **728**, 216 (2014); B. B. Abelev, *et al.* (ALICE Collaboration), **734**, 409 (2014).

[9] A. Andronic, P. Braun-Munzinger, K. Redlich, and J. Stachel, Decoding the phase structure of QCD via particle production at high energy, Nature (London) **561**, 321 (2018).

[10] S. Wheaton and J. Cleymans, THERMUS: A thermal model package for ROOT, Comput. Phys. Commun. **180**, 84 (2009).

[11] V. Vovchenko and H. Stoecker, Thermal-FIST: A package for heavy-ion collisions and hadronic equation of state, Comput. Phys. Commun. **244**, 295 (2019).

[12] J. Adam *et al.* (ALICE Collaboration), Enhanced production of multi-strange hadrons in high-multiplicity proton-proton collisions, Nat. Phys. **13**, 535 (2017).

[13] S. Acharya *et al.* (ALICE Collaboration), Multiplicity dependence of light-flavor hadron production in pp collisions at $\sqrt{s} =$ 7 TeV, Phys. Rev. C **99**, 024906 (2019).

[14] S. Acharya *et al.* (ALICE Collaboration), Multiplicity dependence of (multi-)strange hadron production in proton-proton collisions at $\sqrt{s} = 13$ TeV, Eur. Phys. J. C **80**, 167 (2020).

[15] C. Bierlich *et al.*, A comprehensive guide to the physics and usage of PYTHIA 8.3, SciPost Phys. Codebases **2022**, 8 (2022).

[16] M. Bahr *et al.*, Herwig++ physics and manual, Eur. Phys. J. C **58**, 639 (2008).

[17] J. R. Christiansen and P. Z. Skands, String formation beyond leading colour, J. High Energy Phys. 08 (2015) 003.

[18] J. Bellm *et al.*, Herwig 7.2 release note, Eur. Phys. J. C **80**, 452 (2020).

[19] C. Bierlich, G. Gustafson, L. Lönnblad, and A. Tarasov, Effects of overlapping strings in pp collisions, J. High Energy Phys. 03 (2015) 148.

[20] V. Topor Pop and M. Petrovici, Multiplicity-dependent p_T distributions of identified particles in pp collisions at 7 TeV within the HIJING/$B\bar{B}$ v2.0 model, Phys. Rev. C **98**, 064903 (2018).

[21] V. Vovchenko, B. Dönigus, and H. Stoecker, Canonical statistical model analysis of p–p, p-Pb, and Pb-Pb collisions at energies available at the CERN Large Hadron Collider, Phys. Rev. C **100**, 054906 (2019).

[22] J. Cleymans, P. M. Lo, K. Redlich, and N. Sharma, Multiplicity dependence of (multi)strange baryons in the canonical ensemble with phase shift corrections, Phys. Rev. C **103**, 014904 (2021).

[23] K. Werner, Core-corona separation in ultra-relativistic heavy ion collisions, Phys. Rev. Lett. **98**, 152301 (2007).

[24] Y. Kanakubo, Y. Tachibana, and T. Hirano, Interplay between core and corona components in high-energy nuclear collisions, Phys. Rev. C **105**, 024905 (2022).

[25] K. Aamodt *et al.* (ALICE Collaboration), The ALICE experiment at the CERN LHC, J. Inst. **3**, S08002 (2008).

[26] B. Abelev *et al.* (ALICE Collaboration), Performance of the ALICE experiment at the CERN LHC, Int. J. Mod. Phys. A **29**, 1430044 (2014).

[27] K. Aamodt *et al.* (ALICE Collaboration), Alignment of the ALICE Inner Tracking System with cosmic-ray tracks, J. Inst. **5**, P03003 (2010).

[28] J. Alme *et al.*, The ALICE TPC, a large 3-dimensional tracking device with fast readout for ultra-high multiplicity events, Nucl. Instrum. Methods Phys. Res., Sect. A **622**, 316 (2010).

[29] A. Akindinov *et al.*, Performance of the ALICE Time-of-Flight detector at the LHC, Eur. Phys. J. Plus **128**, 44 (2013).

[30] E. Abbas *et al.* (ALICE Collaboration), Performance of the ALICE VZERO system, J. Instrum. **8**, P10016 (2013).

[31] B. Abelev *et al.* (ALICE Collaboration), Multi-strange baryon production in pp collisions at $\sqrt{s} = 7$ TeV with ALICE, Phys. Lett. B **712**, 309 (2012).

[32] K. Aamodt *et al.* (ALICE Collaboration), Strange particle production in proton-proton collisions at $\sqrt{s} = 0.9$ TeV with ALICE at the LHC, Eur. Phys. J. C **71**, 1594 (2011).

[33] S. Acharya *et al.* (ALICE Collaboration), Pseudorapidity distributions of charged particles as a function of mid- and forward rapidity multiplicities in pp collisions at $\sqrt{s} = 5.02$, 7, and 13 TeV, Eur. Phys. J. C **81**, 630 (2021).

[34] S. Navas *et al.* (Particle Data Group Collaboration), Review of particle physics, Phys. Rev. D **110**, 030001 (2024).

[35] R. Brun, F. Bruyant, F. Carminati, S. Giani, M. Maire, A. McPherson, G. Patrick, and L. Urban, GEANT detector description and simulation tool, CERN-W5013, CERN-W-5013, W5013, W-501.

[36] S. Agostinelli *et al.* (GEANT4 Collaboration), GEANT4 - a simulation toolkit, Nucl. Instrum. Methods Phys. Res., Sect. A **506**, 250 (2003).

[37] C. Tsallis, Possible generalization of Boltzmann-Gibbs statistics, J. Stat. Phys. **52**, 479 (1988).

[38] M. D. Azmi and J. Cleymans, Transverse momentum distributions in proton-proton collisions at LHC energies and Tsallis thermodynamics, J. Phys. G **41**, 065001 (2014).

[39] R. Barlow, Systematic errors: Facts and fictions, in *Conference on Advanced Statistical Techniques in Particle Physics* (University of Durham, Durham, UK, 2002), pp. 134–144 .

[40] C. Loizides and A. Morsch, Apparent strangeness enhancement from multiplicity selection in high energy proton-proton collisions, arXiv:2109.05181.

[41] A. Wald and J. Wolfowitz, On a test whether two samples are from the same population, Ann. Math. Stat. **11**, 147 (1940).

[42] B. Andersson, G. Gustafson, G. Ingelman, and T. Sjostrand, Parton fragmentation and string dynamics, Phys. Rep. **97**, 31 (1983).

[43] T. Sjostrand and M. van Zijl, A multiple interaction model for the event structure in hadron collisions, Phys. Rev. D **36**, 2019 (1987).

[44] K. Werner, Revealing a deep connection between factorization and saturation: New insight into modeling high-energy proton-proton and nucleus-nucleus scattering in the EPOS4 framework, Phys. Rev. C **108**, 064903 (2023).

[45] K. Werner and B. Guiot, Perturbative QCD concerning light and heavy flavor in the EPOS4 framework, Phys. Rev. C **108**, 034904 (2023).

[46] K. Werner, Core-corona procedure and microcanonical hadronization to understand strangeness enhancement in proton-proton and heavy ion collisions in the EPOS4 framework, Phys. Rev. C **109**, 014910 (2024).

[47] H. J. Drescher, M. Hladik, S. Ostapchenko, T. Pierog, and K. Werner, Parton based Gribov-Regge theory, Phys. Rep. **350**, 93 (2001).

[48] Y. Kanakubo, Y. Tachibana, and T. Hirano, Unified description of hadron yield ratios from dynamical core-corona initialization, Phys. Rev. C **101**, 024912 (2020).

[49] ALICE Collaboration, Strangeness production as a function of charged-particle multiplicity in proton-proton collisions at $\sqrt{s} = 5.02$ TeV, HEPData (collection) (2026), https://doi.org/10.17182/hepdata.180658

I. J. Abualrob,[114] S. Acharya,[50] G. Aglieri Rinella,[32] L. Aglietta,[24] N. Agrawal,[25] Z. Ahammed,[134] S. Ahmad,[15] I. Ahuja,[36] Z. Akbar,[81] A. Akindinov,[140] V. Akishina,[38] M. Al-Turany,[96] D. Aleksandrov,[140] B. Alessandro,[56] R. Alfaro Molina,[67] B. Ali,[15] A. Alici,[25,*] A. Alkin,[102] J. Alme,[20] G. Alocco,[24] T. Alt,[64] I. Altsybeev,[94] C. Andrei,[45] N. Andreou,[113] A. Andronic,[125] E. Andronov,[140] M. Angeletti,[32] V. Anguelov,[93] F. Antinori,[54] P. Antonioli,[51] N. Apadula,[72] H. Appelshäuser,[64] S. Arcelli,[25,*] R. Arnaldi,[56] I. C. Arsene,[19] M. Arslandok,[137] A. Augustinus,[32] R. Averbeck,[96] M. D. Azmi,[15] H. Baba,[123] A. R. J. Babu,[136] A. Badalà,[53] J. Bae,[102] Y. Bae,[102] Y. W. Baek,[40] X. Bai,[118] R. Bailhache,[64] Y. Bailung,[48] R. Bala,[90] A. Baldisseri,[129] B. Balis,[2] S. Bangalia,[116] Z. Banoo,[90] V. Barbasova,[36] F. Barile,[31] L. Barioglio,[56] M. Barlou,[24,77] B. Barman,[41] G. G. Barnaföldi,[46] L. S. Barnby,[113] E. Barreau,[101] V. Barret,[126] L. Barreto,[108] K. Barth,[32] E. Bartsch,[64] N. Bastid,[126] G. Batigne,[101] D. Battistini,[94] B. Batyunya,[141] D. Bauri,[47] J. L. Bazo Alba,[100] I. G. Bearden,[82] P. Becht,[96] D. Behera,[48] S. Behera,[47] I. Belikov,[128] V. D. Bella,[128] F. Bellini,[25] R. Bellwied,[114] L. G. E. Beltran,[107] Y. A. V. Beltran,[44] G. Bencedi,[46] A. Bensaoula,[114] S. Beole,[24] Y. Berdnikov,[140] A. Berdnikova,[93] L. Bergmann,[72,93] L. Bernardinis,[23] L. Betev,[32] P. P. Bhaduri,[134] T. Bhalla,[89] A. Bhasin,[90] B. Bhattacharjee,[41] S. Bhattarai,[116] L. Bianchi,[24] J. Bielčík,[34] J. Bielčíková,[85] A. Bilandzic,[94] A. Binoy,[116] G. Biro,[46] S. Biswas,[4] D. Blau,[140] M. B. Blidaru,[96] N. Bluhme,[38] C. Blume,[64] F. Bock,[86] T. Bodova,[20] L. Boldizsár,[46] M. Bombara,[36] P. M. Bond,[32] G. Bonomi,[133,55] H. Borel,[129] A. Borissov,[140] A. G. Borquez Carcamo,[93] E. Botta,[24] Y. E. M. Bouziani,[64] D. C. Brandibur,[63] L. Bratrud,[64] P. Braun-Munzinger,[96] M. Bregant,[108] M. Broz,[34] G. E. Bruno,[95,31] V. D. Buchakchiev,[35] M. D. Buckland,[84] H. Buesching,[64] S. Bufalino,[29] P. Buhler,[74] N. Burmasov,[141] Z. Buthelezi,[68,122] A. Bylinkin,[20] J. C. Cabanillas Noris,[107] M. F. T. Cabrera,[114] H. Caines,[137] A. Caliva,[28] E. Calvo Villar,[100] J. M. M. Camacho,[107] P. Camerini,[23] M. T. Camerlingo,[50] F. D. M. Canedo,[108] S. Cannito,[23] S. L. Cantway,[137] M. Carabas,[111] F. Carnesecchi,[32] C. Carr,[99] L. A. D. Carvalho,[108] J. Castillo Castellanos,[129] M. Castoldi,[32] F. Catalano,[32] S. Cattaruzzi,[23] R. Cerri,[24] I. Chakaberia,[72] P. Chakraborty,[135] J. W. O. Chan,[114] S. Chandra,[134] S. Chapeland,[32] M. Chartier,[117] S. Chattopadhay,[134] M. Chen,[39] T. Cheng,[6] C. Cheshkov,[127] D. Chiappara,[27] V. Chibante Barroso,[32] D. D. Chinellato,[74] F. Chinu,[24] E. S. Chizzali,[94,†] J. Cho,[58] S. Cho,[58] P. Chochula,[32] Z. A. Chochulska,[135,‡] P. Christakoglou,[83] C. H. Christensen,[82] P. Christiansen,[73] T. Chujo,[124] M. Ciacco,[24] C. Cicalo,[52] G. Cimador,[24] F. Cindolo,[51] F. Colamaria,[50] D. Colella,[31] A. Colelli,[31] M. Colocci,[25] M. Concas,[32] G. Conesa Balbastre,[71] Z. Conesa del Valle,[130] G. Contin,[23] J. G. Contreras,[34] M. L. Coquet,[101] P. Cortese,[132,56] M. R. Cosentino,[110] F. Costa,[32] S. Costanza,[21] P. Crochet,[126] M. M. Czarnynoga,[135] A. Dainese,[54] G. Dange,[38] M. C. Danisch,[16] A. Danu,[63] A. Daribayeva,[38] P. Das,[32] S. Das,[4] A. R. Dash,[125] S. Dash,[47] A. De Caro,[28] G. de Cataldo,[50] J. de Cuveland,[38] A. De Falco,[22] D. De Gruttola,[28] N. De Marco,[56] C. De Martin,[23] S. De Pasquale,[28] R. Deb,[133] R. Del Grande,[94] L. Dello Stritto,[32] S. Delsanto,[112] G. G. A. de Souza,[108,§] P. Dhankher,[18] D. Di Bari,[31] M. Di Costanzo,[29] A. Di Mauro,[32] B. Di Ruzza,[131,50,*] B. Diab,[32] Y. Ding,[6] J. Ditzel,[64] R. Divià,[32] U. Dmitrieva,[56] A. Dobrin,[63] B. Dönigus,[64] L. Döpper,[42] J. M. Dubinski,[135] A. Dubla,[96] P. Dupieux,[126] N. Dzalaiova,[13] T. M. Eder,[125] R. J. Ehlers,[72] F. Eisenhut,[64] R. Ejima,[91] D. Elia,[50] B. Erazmus,[101] F. Ercolessi,[25] B. Espagnon,[130] G. Eulisse,[32] D. Evans,[99] L. Fabbietti,[94] G. Fabbri,[51] M. Faggin,[32] J. Faivre,[71] F. Fan,[6] W. Fan,[114] T. Fang,[6] A. Fantoni,[49] M. Fasel,[86] A. Feliciello,[56] W. Feng,[6] G. Feofilov,[140] A. Fernández Téllez,[44] L. Ferrandi,[108] A. Ferrero,[129] C. Ferrero,[56,‖] A. Ferretti,[24] V. J. G. Feuillard,[93] D. Finogeev,[141] F. M. Fionda,[52] A. N. Flores,[106] S. Foertsch,[68] I. Fokin,[93] S. Fokin,[140] U. Follo,[56,‖] R. Forynski,[113] E. Fragiacomo,[57] H. Fribert,[94] J. M. Friedrich,[94] U. Fuchs,[32] N. Funicello,[28] C. Furget,[71] A. Furs,[141] T. Fusayasu,[97] J. J. Gaardhøje,[82] M. Gagliardi,[24] A. M. Gago,[100] T. Gahlaut,[47] C. D. Galvan,[107] S. Gami,[79] P. Ganoti,[77] C. Garabatos,[96] J. M. Garcia,[44] T. García Chávez,[44] E. Garcia-Solis,[9] S. Garetti,[130] C. Gargiulo,[32] P. Gasik,[96] H. M. Gaur,[38] A. Gautam,[116] M. B. Gay Ducati,[66] M. Germain,[101] R. A. Gernhaeuser,[94] C. Ghosh,[134] M. Giacalone,[32] G. Gioachin,[29] S. K. Giri,[134] P. Giubellino,[56] P. Giubilato,[27] P. Glässel,[93] E. Glimos,[121] L. Gonella,[23] V. Gonzalez,[136] M. Gorgon,[2] K. Goswami,[48] S. Gotovac,[33] V. Grabski,[67] L. K. Graczykowski,[135] E. Grecka,[85] A. Grelli,[59] C. Grigoras,[32] V. Grigoriev,[140] S. Grigoryan,[141,1] O. S. Groettvik,[32] F. Grosa,[32] S. Gross-Bölting,[96] J. F. Grosse-Oetringhaus,[32] R. Grosso,[96] D. Grund,[34] N. A. Grunwald,[93] R. Guernane,[71] M. Guilbaud,[101] K. Gulbrandsen,[82] J. K. Gumprecht,[74] T. Gündem,[64] T. Gunji,[123] J. Guo,[10] W. Guo,[6] A. Gupta,[90] R. Gupta,[90] R. Gupta,[48] K. Gwizdziel,[135] L. Gyulai,[46] C. Hadjidakis,[130] F. U. Haider,[90] S. Haidlova,[34] M. Haldar,[4] H. Hamagaki,[75] Y. Han,[139] B. G. Hanley,[136] R. Hannigan,[106] J. Hansen,[73] J. W. Harris,[137] A. Harton,[9] M. V. Hartung,[64] A. Hasan,[120] H. Hassan,[115] D. Hatzifotiadou,[51] P. Hauer,[42] L. B. Havener,[137] E. Hellbär,[32] H. Helstrup,[37] M. Hemmer,[64] S. G. Hernandez,[114] G. Herrera Corral,[8] K. F. Hetland,[37] B. Heybeck,[64] H. Hillemanns,[32] B. Hippolyte,[128] I. P. M. Hobus,[83] F. W. Hoffmann,[38] B. Hofman,[59] Y. Hong,[58] A. Horzyk,[2] Y. Hou,[96,11,6] P. Hristov,[32] P. Huhn,[64] L. M. Huhta,[115] T. J. Humanic,[87] V. Humlova,[34] M. Husar,[88] A. Hutson,[114] D. Hutter,[38] M. C. Hwang,[18] R. Ilkaev,[140] M. Inaba,[124] M. Ippolitov,[140] A. Isakov,[83] T. Isidori,[116] M. S. Islam,[47] M. Ivanov,[13] M. Ivanov,[96] K. E. Iversen,[73] M. Jablonski,[2] B. Jacak,[18,72] N. Jacazio,[25] P. M. Jacobs,[72] A. Jadlovska,[104] S. Jadlovska,[104] S. Jaelani,[81] C. Jahnke,[109] M. J. Jakubowska,[135] E. P. Jamro,[2] D. M. Janik,[34] M. A. Janik,[135] C. A. Jauch,[96] S. Ji,[16] Y. Ji,[96] S. Jia,[82] T. Jiang,[10] A. A. P. Jimenez,[65] S. Jin,[10] F. Jonas,[72] D. M. Jones,[117] J. M. Jowett,[32,96] J. Jung,[64]

M. Jung,[64] A. Junique,[32] A. Jusko,[99] J. Kaewjai,[103] P. Kalinak,[60] A. Kalweit,[32] H. Kang,[12] A. Karasu Uysal,[138] N. Karatzenis,[99] O. Karavichev,[140] T. Karavicheva,[140] M. J. Karwowska,[135] V. Kashyap,[79] M. Keil,[32] B. Ketzer,[42] J. Keul,[64] S. S. Khade,[48] A. M. Khan,[118] A. Khanzadeev,[140] Y. Kharlov,[140] A. Khatun,[116] A. Khuntia,[51] Z. Khuranova,[64] B. Kileng,[37] B. Kim,[102] D. J. Kim,[115] D. Kim,[102] E. J. Kim,[69] G. Kim,[58] H. Kim,[58] J. Kim,[139] J. Kim,[58] J. Kim,[139] J. Kim,[32] M. Kim,[18] S. Kim,[17] T. Kim,[139] K. Kimura,[91] J. T. Kinner,[125] S. Kirsch,[64] I. Kisel,[38] S. Kiselev,[140] A. Kisiel,[135] J. L. Klay,[5] J. Klein,[32] S. Klein,[72] C. Klein-Bösing,[125] M. Kleiner,[64] A. Kluge,[32] M. B. Knuesel,[137] C. Kobdaj,[103] R. Kohara,[123] A. Kondratyev,[141] N. Kondratyeva,[140] J. Konig,[64] P. J. Konopka,[32] G. Kornakov,[135] M. Korwieser,[94] S. D. Koryciak,[2] C. Koster,[83] A. Kotliarov,[85] N. Kovacic,[88] V. Kovalenko,[140] M. Kowalski,[105] V. Kozhuharov,[35] G. Kozlov,[38] I. Králik,[60] A. Kravčáková,[36] L. Krcal,[32] M. Krivda,[60,99] F. Krizek,[85] K. Krizkova Gajdosova,[34] C. Krug,[66] M. Krüger,[64] E. Kryshen,[140] V. Kučera,[58] C. Kuhn,[128] T. Kumaoka,[124] D. Kumar,[134] L. Kumar,[89] N. Kumar,[89] S. Kumar,[50] S. Kundu,[32] M. Kuo,[124] P. Kurashvili,[78] A. B. Kurepin,[140] S. Kurita,[91] A. Kuryakin,[140] S. Kushpil,[85] A. Kuznetsov,[141] M. J. Kweon,[58] Y. Kwon,[139] S. L. La Pointe,[38] P. La Rocca,[26] A. Lakrathok,[103] S. Lambert,[101] A. R. Landou,[71] R. Langoy,[120] P. Larionov,[32] E. Laudi,[32] L. Lautner,[94] R. A. N. Laveaga,[107] R. Lavicka,[74] R. Lea,[133,55] J. B. Lebert,[38] H. Lee,[102] S. Lee,[58] I. Legrand,[45] G. Legras,[125] A. M. Lejeune,[34] T. M. Lelek,[2] I. León Monzón,[107] M. M. Lesch,[94] P. Lévai,[46] M. Li,[6] P. Li,[10] X. Li,[10] B. E. Liang-Gilman,[18] J. Lien,[120] R. Lietava,[99] I. Likmeta,[114] B. Lim,[56] H. Lim,[16] S. H. Lim,[16] S. Lin,[10] V. Lindenstruth,[38] C. Lippmann,[96] D. Liskova,[104] D. H. Liu,[6] J. Liu,[117] Y. Liu,[6] G. S. S. Liveraro,[109] I. M. Lofnes,[20] C. Loizides,[86] S. Lokos,[105] J. Lömker,[59] X. Lopez,[126] E. López Torres,[7] C. Lotteau,[127] P. Lu,[118] W. Lu,[6] Z. Lu,[10] O. Lubynets,[96] F. V. Lugo,[67] J. Luo,[39] G. Luparello,[57] Y. G. Ma,[39] M. Mager,[32] M. Mahlein,[94] A. Maire,[128] E. Majerz,[2] M. V. Makariev,[35] G. Malfattore,[51] N. M. Malik,[90] N. Malik,[15] S. K. Malik,[90] D. Mallick,[130] N. Mallick,[115] G. Mandaglio,[30,53] S. K. Mandal,[78] A. Manea,[63] R. Manhart,[94] V. Manko,[140] A. K. Manna,[48] F. Manso,[126] G. Mantzaridis,[94] V. Manzari,[50] Y. Mao,[6] R. W. Marcjan,[2] G. V. Margagliotti,[23] A. Margotti,[51] A. Marín,[96] C. Markert,[106] P. Martinengo,[32] M. I. Martínez,[44] M. P. P. Martins,[32,108] S. Masciocchi,[96] M. Masera,[24] A. Masoni,[52] L. Massacrier,[130] O. Massen,[59] A. Mastroserio,[131,50] L. Mattei,[24,126] S. Mattiazzo,[27] A. Matyja,[105] J. L. Mayo,[106] F. Mazzaschi,[32] M. Mazzilli,[31,114] Y. Melikyan,[43] M. Melo,[108] A. Menchaca-Rocha,[67] J. E. M. Mendez,[65] E. Meninno,[74] M. W. Menzel,[32,93] M. Meres,[13] L. Micheletti,[56] D. Mihai,[111] D. L. Mihaylov,[94] A. U. Mikalsen,[20] K. Mikhaylov,[141,140] L. Millot,[71] N. Minafra,[116,¶] D. Miśkowiec,[96] A. Modak,[57,133] B. Mohanty,[79] M. Mohisin Khan,[15,**] M. A. Molander,[43] M. M. Mondal,[79] S. Monira,[135] D. A. Moreira De Godoy,[125] A. Morsch,[32] T. Mrnjavac,[32] S. Mrozinski,[64] V. Muccifora,[49] S. Muhuri,[134] A. Mulliri,[22] M. G. Munhoz,[108] R. H. Munzer,[64] L. Musa,[32] J. Musinsky,[60] J. W. Myrcha,[135] B. Naik,[122] A. I. Nambrath,[18] B. K. Nandi,[47] R. Nania,[51] E. Nappi,[50] A. F. Nassirpour,[17] V. Nastase,[111] A. Nath,[93] N. F. Nathanson,[82] K. Naumov,[18] A. Neagu,[19] L. Nellen,[65] R. Nepeivoda,[73] S. Nese,[19] N. Nicassio,[31] B. S. Nielsen,[82] E. G. Nielsen,[82] S. Nikolaev,[140] V. Nikulin,[140] F. Noferini,[51] S. Noh,[12] P. Nomokonov,[141] J. Norman,[117] N. Novitzky,[86] A. Nyanin,[140] J. Nystrand,[20] M. R. Ockleton,[117] M. Ogino,[75] J. Oh,[16] S. Oh,[17] A. Ohlson,[73] M. Oida,[91] V. A. Okorokov,[140] C. Oppedisano,[56] A. Ortiz Velasquez,[65] H. Osanai,[75] J. Otwinowski,[105] M. Oya,[91] K. Oyama,[75] S. Padhan,[133,47] D. Pagano,[133,55] G. Paić,[65] S. Paisano-Guzmán,[44] A. Palasciano,[95,50] I. Panasenko,[73] P. Panigrahi,[47] C. Pantouvakis,[27] H. Park,[124] J. Park,[124] S. Park,[102] T. Y. Park,[139] J. E. Parkkila,[135] P. B. Pati,[82] Y. Patley,[47] R. N. Patra,[50] P. Paudel,[116] B. Paul,[134] H. Pei,[6] T. Peitzmann,[59] X. Peng,[54,11] M. Pennisi,[24] S. Perciballi,[24] D. Peresunko,[140] G. M. Perez,[7] Y. Pestov,[140] M. Petrovici,[45] S. Piano,[57] M. Pikna,[13] P. Pillot,[101] O. Pinazza,[51,32] C. Pinto,[32] S. Pisano,[49] M. Płoskoń,[72] M. Planinic,[88] D. K. Plociennik,[2] M. G. Poghosyan,[86] B. Polichtchouk,[140] S. Politano,[32] N. Poljak,[88] A. Pop,[45] S. Porteboeuf-Houssais,[126] J. S. Potgieter,[112] I. Y. Pozos,[44] K. K. Pradhan,[48] S. K. Prasad,[4] S. Prasad,[48] R. Preghenella,[51] F. Prino,[56] C. A. Pruneau,[136] I. Pshenichnov,[140] M. Puccio,[32] S. Pucillo,[28,24] S. Pulawski,[119] L. Quaglia,[24] A. M. K. Radhakrishnan,[48] S. Ragoni,[14] A. Rai,[137] A. Rakotozafindrabe,[129] N. Ramasubramanian,[127] L. Ramello,[132,56] C. O. Ramírez-Álvarez,[44] M. Rasa,[26] S. S. Räsänen,[43] R. Rath,[96] M. P. Rauch,[20] I. Ravasenga,[32] M. Razza,[25] K. F. Read,[86,121] C. Reckziegel,[110] A. R. Redelbach,[38] K. Redlich,[78,††] H. D. Regules-Medel,[44] A. Rehman,[20] F. Reidt,[32] H. A. Reme-Ness,[37] K. Reygers,[93] R. Ricci,[28] M. Richter,[20] A. A. Riedel,[94] W. Riegler,[32] A. G. Riffero,[24] M. Rignanese,[27] C. Ripoli,[28] C. Ristea,[63] M. V. Rodriguez,[32] M. Rodríguez Cahuantzi,[44] K. Røed,[19] R. Rogalev,[140] E. Rogochaya,[141] D. Rohr,[32] D. Röhrich,[20] S. Rojas Torres,[34] P. S. Rokita,[135] G. Romanenko,[25] F. Ronchetti,[32] D. Rosales Herrera,[44] K. Roslon,[135] A. Rossi,[54] A. Roy,[48] S. Roy,[47] N. Rubini,[51] J. A. Rudolph,[83] D. Ruggiano,[135] R. Rui,[23] P. G. Russek,[2] A. Rustamov,[80] Y. Ryabov,[140] A. Rybicki,[105] L. C. V. Ryder,[116] G. Ryu,[70] J. Ryu,[16] W. Rzesa,[94,135] B. Sabiu,[51] R. Sadek,[72] S. Sadhu,[42] S. Sadovsky,[140] A. Saha,[31] S. Saha,[79] B. Sahoo,[48] R. Sahoo,[48] D. Sahu,[65] P. K. Sahu,[61] J. Saini,[134] S. Sakai,[124] S. Sambyal,[90] D. Samitz,[74] I. Sanna,[32] T. B. Saramela,[108] D. Sarkar,[82] V. Sarritzu,[22] V. M. Sarti,[94] U. Savino,[24] S. Sawan,[79] E. Scapparone,[51] J. Schambach,[86] H. S. Scheid,[32] C. Schiaua,[45] R. Schicker,[93] F. Schlepper,[32,93] A. Schmah,[96] C. Schmidt,[96] M. Schmidt,[92] N. V. Schmidt,[86] J. Schoengarth,[64] R. Schotter,[74] A. Schröter,[38] J. Schukraft,[32] K. Schweda,[96] G. Scioli,[25] E. Scomparin,[56]

J. E. Seger,[14] Y. Sekiguchi,[123] D. Sekihata,[123] M. Selina,[83] I. Selyuzhenkov,[96] S. Senyukov,[128] J. J. Seo,[93] D. Serebryakov,[140] L. Serkin,[65,‡‡] L. Šerkšnytė,[94] A. Sevcenco,[63] T. J. Shaba,[68] A. Shabetai,[101] R. Shahoyan,[32] B. Sharma,[90] D. Sharma,[47] H. Sharma,[54] M. Sharma,[90] S. Sharma,[90] T. Sharma,[41] U. Sharma,[90] O. Sheibani,[136] K. Shigaki,[91] M. Shimomura,[76] S. Shirinkin,[140] Q. Shou,[39] Y. Sibiriak,[140] S. Siddhanta,[52] T. Siemiarczuk,[78] T. F. Silva,[108] W. D. Silva,[108] D. Silvermyr,[73] T. Simantathammakul,[103] R. Simeonov,[35] B. Singh,[90] B. Singh,[94] K. Singh,[48] R. Singh,[79] R. Singh,[54,96] S. Singh,[15] V. K. Singh,[134] V. Singhal,[134] T. Sinha,[98] B. Sitar,[13] M. Sitta,[132,56] T. B. Skaali,[19] G. Skorodumovs,[93] N. Smirnov,[137] K. L. Smith,[16] R. J. M. Snellings,[59] E. H. Solheim,[19] C. Sonnabend,[32,96] J. M. Sonneveld,[83] F. Soramel,[27] A. B. Soto-Hernandez,[87] R. Spijkers,[83] C. Sporleder,[115] I. Sputowska,[105] J. Staa,[73] J. Stachel,[93] L. L. Stahl,[108] I. Stan,[63] T. Stellhorn,[125] S. F. Stiefelmaier,[93] D. Stocco,[101] I. Storehaug,[19] N. J. Strangmann,[64] P. Stratmann,[125] S. Strazzi,[25] A. Sturniolo,[30,53] Y. Su,[6] A. A. P. Suaide,[108] C. Suire,[130] A. Suiu,[111] M. Sukhanov,[141] M. Suljic,[32] R. Sultanov,[140] V. Sumberia,[90] S. Sumowidagdo,[81] N. B. Sundstrom,[59] L. H. Tabares,[7] S. F. Taghavi,[94] J. Takahashi,[109] M. A. Talamantes Johnson,[44] G. J. Tambave,[79] Z. Tang,[118] J. Tanwar,[89] J. D. Tapia Takaki,[116] N. Tapus,[111] L. A. Tarasovicova,[36] M. G. Tarzila,[45] A. Tauro,[32] A. Tavira García,[130] G. Tejeda Muñoz,[44] L. Terlizzi,[24] C. Terrevoli,[50] D. Thakur,[24] S. Thakur,[4] M. Thogersen,[19] D. Thomas,[106] N. Tiltmann,[32,125] A. R. Timmins,[114] A. Toia,[64] R. Tokumoto,[91] S. Tomassini,[25] K. Tomohiro,[91] Q. Tong,[6] N. Topilskaya,[140] V. V. Torres,[101] A. Trifiró,[30,53] T. Triloki,[95] A. S. Triolo,[32,53] S. Tripathy,[32] T. Tripathy,[126] S. Trogolo,[24] V. Trubnikov,[3] W. H. Trzaska,[115] T. P. Trzcinski,[135] C. Tsolanta,[19] R. Tu,[39] A. Tumkin,[140] R. Turrisi,[54] T. S. Tveter,[19] K. Ullaland,[20] B. Ulukutlu,[94] S. Upadhyaya,[105] A. Uras,[127] M. Urioni,[23] G. L. Usai,[22] M. Vaid,[90] M. Vala,[36] N. Valle,[55] L. V. R. van Doremalen,[59] M. van Leeuwen,[83] C. A. van Veen,[93] R. J. G. van Weelden,[83] D. Varga,[46] Z. Varga,[137] P. Vargas Torres,[65] M. Vasileiou,[77] O. Vázquez Doce,[49] O. Vazquez Rueda,[114] V. Vechernin,[140] P. Veen,[129] E. Vercellin,[24] R. Verma,[47] R. Vértesi,[46] M. Verweij,[59] L. Vickovic,[33] Z. Vilakazi,[122] A. Villani,[23] C. J. D. Villiers,[68] A. Vinogradov,[140] T. Virgili,[28] M. M. O. Virta,[115] A. Vodopyanov,[141] M. A. Völkl,[99] S. A. Voloshin,[136] G. Volpe,[31] B. von Haller,[32] I. Vorobyev,[32] N. Vozniuk,[141] J. Vrláková,[36] J. Wan,[39] C. Wang,[39] D. Wang,[39] Y. Wang,[118] Y. Wang,[39] Y. Wang,[6] Z. Wang,[39] F. Weiglhofer,[32,38] S. C. Wenzel,[32] J. P. Wessels,[125] P. K. Wiacek,[2] J. Wiechula,[64] J. Wikne,[19] G. Wilk,[78] J. Wilkinson,[96] G. A. Willems,[125] B. Windelband,[93] J. Witte,[93] M. Wojnar,[2] J. R. Wright,[106] C.-T. Wu,[6,27] W. Wu,[94,39] Y. Wu,[118] K. Xiong,[39] Z. Xiong,[118] L. Xu,[127,6] R. Xu,[6] A. Yadav,[42] A. K. Yadav,[134] Y. Yamaguchi,[91] S. Yang,[58] S. Yang,[20] S. Yano,[91] Z. Ye,[72] E. R. Yeats,[18] J. Yi,[6] R. Yin,[39] Z. Yin,[6] I.-K. Yoo,[16] J. H. Yoon,[58] H. Yu,[12] S. Yuan,[20] A. Yuncu,[93] V. Zaccolo,[23] C. Zampolli,[32] F. Zanone,[93] N. Zardoshti,[32] P. Závada,[62] B. Zhang,[93] C. Zhang,[129] L. Zhang,[39] M. Zhang,[126,6] M. Zhang,[27,6] S. Zhang,[39] X. Zhang,[6] Y. Zhang,[118] Y. Zhang,[118] Z. Zhang,[6] V. Zherebchevskii,[140] Y. Zhi,[10] D. Zhou,[6] Y. Zhou,[82] J. Zhu,[39] S. Zhu,[96,118] Y. Zhu,[6] A. Zingaretti,[27] S. C. Zugravel,[56] and N. Zurlo[133,55]

(ALICE Collaboration)

[1]*A.I. Alikhanyan National Science Laboratory (Yerevan Physics Institute) Foundation, Yerevan, Armenia*
[2]*AGH University of Krakow, Cracow, Poland*
[3]*Bogolyubov Institute for Theoretical Physics, National Academy of Sciences of Ukraine, Kyiv, Ukraine*
[4]*Bose Institute, Department of Physics and Centre for Astroparticle Physics and Space Science (CAPSS), Kolkata, India*
[5]*California Polytechnic State University, San Luis Obispo, California, USA*
[6]*Central China Normal University, Wuhan, China*
[7]*Centro de Aplicaciones Tecnológicas y Desarrollo Nuclear (CEADEN), Havana, Cuba*
[8]*Centro de Investigación y de Estudios Avanzados (CINVESTAV), Mexico City and Mérida, Mexico*
[9]*Chicago State University, Chicago, Illinois, USA*
[10]*China Nuclear Data Center, China Institute of Atomic Energy, Beijing, China*
[11]*China University of Geosciences, Wuhan, China*
[12]*Chungbuk National University, Cheongju, Republic of Korea*
[13]*Comenius University Bratislava, Faculty of Mathematics, Physics and Informatics, Bratislava, Slovak Republic*
[14]*Creighton University, Omaha, Nebraska, USA*
[15]*Department of Physics, Aligarh Muslim University, Aligarh, India*
[16]*Department of Physics, Pusan National University, Pusan, Republic of Korea*
[17]*Department of Physics, Sejong University, Seoul, Republic of Korea*
[18]*Department of Physics, University of California, Berkeley, California, USA*
[19]*Department of Physics, University of Oslo, Oslo, Norway*
[20]*Department of Physics and Technology, University of Bergen, Bergen, Norway*
[21]*Dipartimento di Fisica, Università di Pavia, Pavia, Italy*
[22]*Dipartimento di Fisica dell'Università and Sezione INFN, Cagliari, Italy*
[23]*Dipartimento di Fisica dell'Università and Sezione INFN, Trieste, Italy*

[24]*Dipartimento di Fisica dell'Università and Sezione INFN, Turin, Italy*
[25]*Dipartimento di Fisica e Astronomia dell'Università and Sezione INFN, Bologna, Italy*
[26]*Dipartimento di Fisica e Astronomia dell'Università and Sezione INFN, Catania, Italy*
[27]*Dipartimento di Fisica e Astronomia dell'Università and Sezione INFN, Padova, Italy*
[28]*Dipartimento di Fisica 'E.R. Caianiello' dell'Università and Gruppo Collegato INFN, Salerno, Italy*
[29]*Dipartimento DISAT del Politecnico and Sezione INFN, Turin, Italy*
[30]*Dipartimento di Scienze MIFT, Università di Messina, Messina, Italy*
[31]*Dipartimento Interateneo di Fisica 'M. Merlin' and Sezione INFN, Bari, Italy*
[32]*European Organization for Nuclear Research (CERN), Geneva, Switzerland*
[33]*Faculty of Electrical Engineering, Mechanical Engineering and Naval Architecture, University of Split, Split, Croatia*
[34]*Faculty of Nuclear Sciences and Physical Engineering, Czech Technical University in Prague, Prague, Czech Republic*
[35]*Faculty of Physics, Sofia University, Sofia, Bulgaria*
[36]*Faculty of Science, P.J. Šafárik University, Košice, Slovak Republic*
[37]*Faculty of Technology, Environmental and Social Sciences, Bergen, Norway*
[38]*Frankfurt Institute for Advanced Studies, Johann Wolfgang Goethe-Universität Frankfurt, Frankfurt, Germany*
[39]*Fudan University, Shanghai, China*
[40]*Gangneung-Wonju National University, Gangneung, Republic of Korea*
[41]*Gauhati University, Department of Physics, Guwahati, India*
[42]*Helmholtz-Institut für Strahlen- und Kernphysik, Rheinische Friedrich-Wilhelms-Universität Bonn, Bonn, Germany*
[43]*Helsinki Institute of Physics (HIP), Helsinki, Finland*
[44]*High Energy Physics Group, Universidad Autónoma de Puebla, Puebla, Mexico*
[45]*Horia Hulubei National Institute of Physics and Nuclear Engineering, Bucharest, Romania*
[46]*HUN-REN Wigner Research Centre for Physics, Budapest, Hungary*
[47]*Indian Institute of Technology Bombay (IIT), Mumbai, India*
[48]*Indian Institute of Technology Indore, Indore, India*
[49]*INFN, Laboratori Nazionali di Frascati, Frascati, Italy*
[50]*INFN, Sezione di Bari, Bari, Italy*
[51]*INFN, Sezione di Bologna, Bologna, Italy*
[52]*INFN, Sezione di Cagliari, Cagliari, Italy*
[53]*INFN, Sezione di Catania, Catania, Italy*
[54]*INFN, Sezione di Padova, Padova, Italy*
[55]*INFN, Sezione di Pavia, Pavia, Italy*
[56]*INFN, Sezione di Torino, Turin, Italy*
[57]*INFN, Sezione di Trieste, Trieste, Italy*
[58]*Inha University, Incheon, Republic of Korea*
[59]*Institute for Gravitational and Subatomic Physics (GRASP), Utrecht University/Nikhef, Utrecht, Netherlands*
[60]*Institute of Experimental Physics, Slovak Academy of Sciences, Košice, Slovak Republic*
[61]*Institute of Physics, Homi Bhabha National Institute, Bhubaneswar, India*
[62]*Institute of Physics of the Czech Academy of Sciences, Prague, Czech Republic*
[63]*Institute of Space Science (ISS), Bucharest, Romania*
[64]*Institut für Kernphysik, Johann Wolfgang Goethe-Universität Frankfurt, Frankfurt, Germany*
[65]*Instituto de Ciencias Nucleares, Universidad Nacional Autónoma de México, Mexico City, Mexico*
[66]*Instituto de Física, Universidade Federal do Rio Grande do Sul (UFRGS), Porto Alegre, Brazil*
[67]*Instituto de Física, Universidad Nacional Autónoma de México, Mexico City, Mexico*
[68]*iThemba LABS, National Research Foundation, Somerset West, South Africa*
[69]*Jeonbuk National University, Jeonju, Republic of Korea*
[70]*Korea Institute of Science and Technology Information, Daejeon, Republic of Korea*
[71]*Laboratoire de Physique Subatomique et de Cosmologie, Université Grenoble-Alpes, CNRS-IN2P3, Grenoble, France*
[72]*Lawrence Berkeley National Laboratory, Berkeley, California, USA*
[73]*Lund University Department of Physics, Division of Particle Physics, Lund, Sweden*
[74]*Marietta Blau Institute, Vienna, Austria*
[75]*Nagasaki Institute of Applied Science, Nagasaki, Japan*
[76]*Nara Women's University (NWU), Nara, Japan*
[77]*National and Kapodistrian University of Athens, School of Science, Department of Physics, Athens, Greece*
[78]*National Centre for Nuclear Research, Warsaw, Poland*
[79]*National Institute of Science Education and Research, Homi Bhabha National Institute, Jatni, India*
[80]*National Nuclear Research Center, Baku, Azerbaijan*
[81]*National Research and Innovation Agency - BRIN, Jakarta, Indonesia*
[82]*Niels Bohr Institute, University of Copenhagen, Copenhagen, Denmark*

[83] Nikhef, National institute for subatomic physics, Amsterdam, Netherlands
[84] Nuclear Physics Group, STFC Daresbury Laboratory, Daresbury, United Kingdom
[85] Nuclear Physics Institute of the Czech Academy of Sciences, Husinec-Řež, Czech Republic
[86] Oak Ridge National Laboratory, Oak Ridge, Tennessee, USA
[87] Ohio State University, Columbus, Ohio, USA
[88] Physics department, Faculty of science, University of Zagreb, Zagreb, Croatia
[89] Physics Department, Panjab University, Chandigarh, India
[90] Physics Department, University of Jammu, Jammu, India
[91] Physics Program and International Institute for Sustainability with Knotted Chiral Meta Matter (WPI-SKCM^2), Hiroshima University, Hiroshima, Japan
[92] Physikalisches Institut, Eberhard-Karls-Universität Tübingen, Tübingen, Germany
[93] Physikalisches Institut, Ruprecht-Karls-Universität Heidelberg, Heidelberg, Germany
[94] Physik Department, Technische Universität München, Munich, Germany
[95] Politecnico di Bari and Sezione INFN, Bari, Italy
[96] Research Division and ExtreMe Matter Institute EMMI, GSI Helmholtzzentrum für Schwerionenforschung GmbH, Darmstadt, Germany
[97] Saga University, Saga, Japan
[98] Saha Institute of Nuclear Physics, Homi Bhabha National Institute, Kolkata, India
[99] School of Physics and Astronomy, University of Birmingham, Birmingham, United Kingdom
[100] Sección Física, Departamento de Ciencias, Pontificia Universidad Católica del Perú, Lima, Peru
[101] SUBATECH, IMT Atlantique, Nantes Université, CNRS-IN2P3, Nantes, France
[102] Sungkyunkwan University, Suwon City, Republic of Korea
[103] Suranaree University of Technology, Nakhon Ratchasima, Thailand
[104] Technical University of Košice, Košice, Slovak Republic
[105] The Henryk Niewodniczanski Institute of Nuclear Physics, Polish Academy of Sciences, Cracow, Poland
[106] The University of Texas at Austin, Austin, Texas, USA
[107] Universidad Autónoma de Sinaloa, Culiacán, Mexico
[108] Universidade de São Paulo (USP), São Paulo, Brazil
[109] Universidade Estadual de Campinas (UNICAMP), Campinas, Brazil
[110] Universidade Federal do ABC, Santo Andre, Brazil
[111] Universitatea Nationala de Stiinta si Tehnologie Politehnica Bucuresti, Bucharest, Romania
[112] University of Cape Town, Cape Town, South Africa
[113] University of Derby, Derby, United Kingdom
[114] University of Houston, Houston, Texas, USA
[115] University of Jyväskylä, Jyväskylä, Finland
[116] University of Kansas, Lawrence, Kansas, USA
[117] University of Liverpool, Liverpool, United Kingdom
[118] University of Science and Technology of China, Hefei, China
[119] University of Silesia in Katowice, Katowice, Poland
[120] University of South-Eastern Norway, Kongsberg, Norway
[121] University of Tennessee, Knoxville, Tennessee, USA
[122] University of the Witwatersrand, Johannesburg, South Africa
[123] University of Tokyo, Tokyo, Japan
[124] University of Tsukuba, Tsukuba, Japan
[125] Universität Münster, Institut für Kernphysik, Münster, Germany
[126] Université Clermont Auvergne, CNRS/IN2P3, LPC, Clermont-Ferrand, France
[127] Université de Lyon, CNRS/IN2P3, Institut de Physique des 2 Infinis de Lyon, Lyon, France
[128] Université de Strasbourg, CNRS, IPHC UMR 7178, F-67000 Strasbourg, France, Strasbourg, France
[129] Université Paris-Saclay, Centre d'Etudes de Saclay (CEA), IRFU, Département de Physique Nucléaire (DPhN), Saclay, France
[130] Université Paris-Saclay, CNRS/IN2P3, IJCLab, Orsay, France
[131] Università degli Studi di Foggia, Foggia, Italy
[132] Università del Piemonte Orientale, Vercelli, Italy
[133] Università di Brescia, Brescia, Italy
[134] Variable Energy Cyclotron Centre, Homi Bhabha National Institute, Kolkata, India
[135] Warsaw University of Technology, Warsaw, Poland
[136] Wayne State University, Detroit, Michigan, USA
[137] Yale University, New Haven, Connecticut, USA
[138] Yildiz Technical University, Istanbul, Turkey
[139] Yonsei University, Seoul, Republic of Korea

[140]*Affiliated with an institute formerly covered by a cooperation agreement with CERN*
[141]*Affiliated with an international laboratory covered by a cooperation agreement with CERN*

[*]Deceased.
[†]Also at Max-Planck-Institut fur Physik, Munich, Germany.
[‡]Also at Czech Technical University in Prague, Prague, Czech Republic.
[§]Also at Instituto de Fisica da Universidade de Sao Paulo.
[‖]Also at Dipartimento DET del Politecnico di Torino, Turin, Italy.
[¶]Also at University College of Dublin, Dublin, Ireland.
[**]Also at Department of Applied Physics, Aligarh Muslim University, Aligarh, India.
[††]Also at Institute of Theoretical Physics, University of Wroclaw, Wroclaw, Poland.
[‡‡]Also at Facultad de Ciencias, Universidad Nacional Autónoma de México, Mexico City, Mexico.